Thermal fluctuations in supercrystal stripe phases of Langmuir monolayers

A. Deutsch and S. A. Safran
Department of Materials and Interfaces, The Weizmann Institute of Science, Rehovot 76100, Israel
(Received 11 December 1995)

We predict the magnitude of fluctuations of two-dimensional, supercrystal stripe phases of Langmuir monolayers, composed of polar molecules, in the low temperature regime. Our model includes both the microscopic line tension and the interdomain, long-range dipolar interactions. We calculate (in the long wavelength approximation) the elastic energy of the stripes and show that the stripes exhibit long-range orientational order. We predict that the stabilization of the stripe width by the dipolar interactions tends to decrease the thermal roughness of the domain walls compared with systems with only short-range interactions. In the case of crystalline stripes our results suggest a possible finite-temperature first-order roughening transition. [S1063-651X(96)13809-5]

PACS number(s): 68.10.−m, 68.60.Dv, 68.15.+e, 64.70.−p

I. INTRODUCTION

A variety of amphiphile molecules (surfactants, fatty acids, or lipids) form insoluble monolayers at the water/air interface (Langmuir monolayers). The phase diagrams of these systems have been extensively studied and show a wide variety of behaviors (see, for example, Refs. [1–3]) such as the coexistence of liquid-gas or liquid-expanded–liquid-condensed phases with very large domains. When the molecules that form such monolayers carry a permanent electric dipolar moment, an even richer phase diagram was predicted theoretically [4–7]. The competition between the short-range attractions (due to van der Waals interactions) and the long-range dipolar repulsion favors spatial inhomogeneities of the in-plane molecular concentration and results in the formation of various mesoscopic structures including macroscopic modulated phases such as ordered stripe or bubble phases. This behavior is also shared by other quasi-two-dimensional systems with dipolar interactions, such as magnetic thin films.

In the present work, we study both equilibrium properties and thermal fluctuations of the domains in the stripe phase, and predict the orientational ordering and roughening of the stripes.

We consider monolayers which consist of a single type of molecule that carries a permanent dipolar moment perpendicular to the flat interface (for the treatment of in-plane dipoles see, for example, Ref. [8]). In such systems, the dipolar interaction between two molecules reduces to $\sim P^2/r^3$, where $\vec{P}$ is the dipolar moment of a molecule and r is the distance between the molecules. We discard effects arising from internal degrees of freedoms of the molecules, such as the tilt of the tails [9], and study a system with uniaxial modulation of the molecular density in the low-temperature regime. In this regime, far from the critical temperature for the onset of the modulation, domain walls are sharp and the resulting supercrystal stripe phase is composed of two alternating homogeneous stripes 1,2 with dipolar densities σ_1 and σ_2, respectively.

Our results are described in terms of four physical parameters: (i) $\mu^2 \equiv (\sigma_1 - \sigma_2)^2 K_d$, where $K_d \sim P^2$ is the dipolar interaction strength, which is very sensitive to the dielectric properties of the system [5]; (ii) the microscopic cutoff Δ, which is approximately the intermolecular distance; (iii) the microscopic isotropic line tension γ, that accounts for the short-range attractions; and (iv) the surface fraction of the phases $\phi \equiv \phi_1 = 1 - \phi_2$. Our formal analysis is valid for $0 \leqslant \phi \leqslant 1$, but we stress that the variation of the surface fraction ϕ may induce phase transition to other phases (e.g., bubble phase, as suggested by Ref. [10]).

In our review of the well-established equilibrium analysis of the stripe phase [4,5,11,12] we recalculate the stripe periodicity with a new emphasis on the energy scales of the system. We find that the self-energy of a minority phase stripe (the smaller of ϕ_1 and ϕ_2) is much larger than its interaction energy with distant stripes. This results in a relatively fixed width of the minority phase stripes, which very weakly depends on the surface fraction ϕ. We thus find that the main response of the system to a change in the surface fraction is to adjust the period of the supercrystal rather than the width of the stripes. This result is also relevant to the calculations of the fluctuations in the stripe width, which we find to be very small on the scale of the stripe width (although it is usually large enough to roughen the domain walls; see below).

Fluctuations of the stripe phase were previously considered in the literature using two main approaches. The first one is phenomenological and starts from a continuum model of the displacements of the stripes, which leads to an elastic Hamiltonian [13–15]. The second one uses exact calculations for infinite wavelength *collective* modes of the stripes (i.e., all the boundaries of the stripes fluctuate identically), mainly for stability analysis of the phase [10,16–18]. In our work, we bridge the two approaches and calculate (to second order in the fluctuations) the *full* fluctuation Hamiltonian of the stripes, which leads to acoustic and optical branches in the energy spectrum. Our results for the fluctuation energy spectrum are similar to those of Ref. [19] for thin magnetic films, but we also focus on the effects of these modes in determining the smectic order of the phase and the roughness of the domain boundaries.

At surface fraction $\phi \neq \frac{1}{2}$ we use a simplified physical model and quantify the smectic order of the stripe phase. We

describe the stripes as fluctuating objects with a fixed width (i.e., symmetric fluctuation modes). We find that the system is governed in the long-wavelength approximation by an elastic Hamiltonian and obtain simple analytic expressions for the bending and compression moduli.

We find that the symmetric fluctuation modes of the stripes can have large amplitudes, which results in a failure of our second-order (harmonic) approximation for the fluctuation Hamiltonian at large length scales. However, we find that the harmonic approximation of the Hamiltonian *is* appropriate to describe the orientational order of the stripe phase. We consider the normal to the stripe boundary $\hat{n}(x)$ and calculate the normal-normal correlation function, $g_n(x)=\langle|\hat{\mathbf{n}}(x)-\hat{\mathbf{n}}(0)|^2\rangle$. We find that normals to the boundary of the same stripe are highly correlated at all length scales. This result implies that the stripe phase exhibits long-range orientational order and that the smectic structure persists over large length scales. A more accurate physical picture is obtained by considering higher orders [20] in the fluctuation amplitude; however, we expect, according to our result, that the orientational order of the phase is long ranged in the more detailed theory as well.

It has been shown by other authors [15,20] that, in such two-dimensional (2D) systems, free dislocations are present at any finite temperature. The finite dislocation density, n_D, results in blobs of area ξ_D^2 which are free of dislocations. Combining this result with the one we obtain implies that within the blobs the smectic structure persists. This physical picture may fail, however, when the size of the blobs is comparable with the stripe periodicity, since then one can no longer refer to a supercrystal structure. Our result also implies that the dislocations, rather than the fluctuations of the stripe boundaries, lead to the destruction of the supercrystal phase at higher temperatures.

This simplified model is supported by our calculation of the roughness of the stripe boundaries (the mean square fluctuations of the stripe width), using a mean field approximation. These width fluctuations are important both for liquid and solid stripes. In the case of a surface of a solid, the mean square of the fluctuations ($\langle y^2\rangle$) determines whether the surface is rough or faceted (nonrough). In a liquid/gas interface the dynamics of these fluctuations are important for the behavior of capillary waves. We find two scaling regimes for the mean square fluctuations of the stripe width: (a) the high-temperature regime, where $\langle y^2\rangle\sim D_m\Delta$ and D_m is the equilibrium width of the minority stripes; and (b) the low-temperature regime, where $\langle y^2\rangle\sim\Delta^2$. The appropriate scaling regime is determined by the dimensionless parameter $\sim T/\mu^2\Delta$. In both regimes we find $\langle y^2\rangle\ll D_m^2$, in agreement with our fixed stripe-width model. For the solid stripe case, we find in regime (b) that, in contrast with two-dimensional systems with only short-range interactions, where the roughening temperature is zero, the long-range dipolar interactions may induce faceting in the stripe boundaries at a finite temperature, via a first-order phase transition. We note that even in regime (a) the stripe boundaries are not strictly speaking rough. The dipolar interactions, which give rise to the supercrystal order, result in an additional restoring force acting on the stripe one-dimensional interface. This restoring force reduces the mean square fluctuations by a macroscopic factor relative to a free liquid interface.

An outline of the paper follows: We start in Sec. II with a review of previous work on the equilibrium properties of the stripe phase with a new emphasis on the energy scales of the system. Our main results are presented in Secs. III and IV. In Sec. III we present our fixed stripe-width model and consider the symmetric fluctuation modes of stripes. Using this model we quantify the smectic order of the system. Section IV discusses the fluctuations of the stripe width and the roughness of a stripe boundary. In the case of a solid stripe we present a self-consistent calculation that predicts a first-order roughening transition.

While we have focused on the essential results in the text, many of the calculations are contained in the appendixes. In Appendix A, we develop the necessary formalism for the analysis of two-dimensional systems with power-law interactions. Using Green's theorem we transform the two-dimensional system to a physical picture of interacting domain boundaries. Appendix B contains the derivation of the interaction energy between two such fluctuating boundaries for the general case of a power-law interaction. We use this formalism specifically for dipolar interactions in the analysis of the stripe phase. In Appendix C we present the normal mode harmonic analysis of the stripe phase, resulting in acoustic and optical branches in the fluctuation energy spectrum. A powerful mathematical tool is developed in Appendix E, where we find a general mathematical relation between the discrete and continuous Fourier transforms of a function, of which the Poisson summation formula is a special case. This relation is used to extend the general wavevector Q dependence of a discrete Fourier transform $\mathcal{F}(Q)$ from $\mathcal{F}(Q=0)$. This method may be used to extend some of the results that appear already in the literature concerning *collective* modes of stripe phases.

II. THE STRIPE PHASE IN EQUILIBRIUM

In order to better understand the fluctuating stripe phase, we review in this section with some modifications and emphasis on the relative energy scales, the well-established analysis of this phase in equilibrium [4,5,11,12]. We consider a system of molecules that interact through a dipolar repulsion and a short-range attraction (e.g., van der Waals interaction). It was shown that in such systems, in equilibrium, the competition between the long-range repulsion and the short-range attraction may give rise to modulation in the surface molecular density (i.e., supercrystal phases).

We consider a one-dimensional supercrystal stripe phase in the low-temperature regime where the domain walls are sharp and where all entropic effects are included in the line tension γ. As shown in Fig. 1, the phase has a period $D=D_1+D_2$ and the unit cell has a basis of two stripes labeled 1,2 with dipolar densities σ_1 and σ_2, respectively. The surface fraction of the stripes labeled 1 is $\phi=D_1/D$, where the parameter D_1, which is the width of the stripes labeled 1, is determined by the composition and the equation of state. The size of the system in the direction parallel to the stripes is denoted L. We use the notation (j,m) to label the stripes where j is the cell index and $m=1,2$ is the index of the stripe within the cell. Using Eq. (A11) the dipolar potential is written $V_{dip}=K_d\rho^{-3}$, where K_d is the interaction

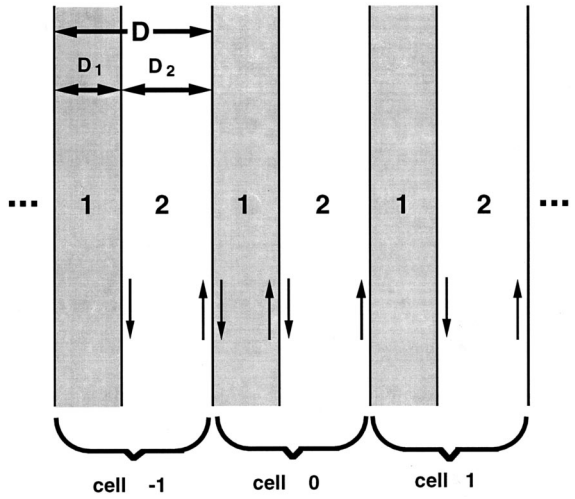

FIG. 1. The stripe phase in equilibrium. This supercrystal phase is composed of alternating stripe domains, labeled 1,2, with dipolar densities σ_1 and σ_2, respectively. The supercrystal has a period $D=D_1+D_2$ and its unit cell contains two stripes (1,2). The cells are labeled $0,\pm1,\pm2,\ldots$. The arrows indicate the ''polarities'' of the boundaries (i.e., the directions in which the line integrals are taken along the boundaries of the stripes) for the calculation of the dipolar energy in Eq. (A13).

strength. We denote as $V(R)$ the spatial dependence of the potential

$$V(R)=\frac{1}{\rho^3}, \tag{2.1}$$

where $\rho=(R^2+\Delta^2)^{1/2}$ and Δ is the microscopic cutoff [21,22]. The electrostatic part of the energy per cell is written

$$\begin{aligned} E_{cell}=&\frac{1}{2}\sum_{m,n=1}^{2}\sum_{j=-\infty}^{\infty}\sigma_m\sigma_n K_d \\ &\times\int_{(0,m)}\int_{(j,n)}d^2r_{(0,m)}d^2r_{(j,n)}V(|\vec{r}_{(0,m)}-\vec{r}_{(j,n)}|) \\ =&\epsilon_1 S_1+\epsilon_2 S_2 \\ &-\tfrac{1}{2}\mu^2\sum_{j=-\infty}^{\infty}\int_{(0,1)}\int_{(j,2)}d^2r_{(0,1)}d^2r_{(j,2)}V(|\vec{r}_{(0,1)}-\vec{r}_{(j,2)}|), \end{aligned} \tag{2.2}$$

where $\epsilon_i=\pi K_d\sigma_i^2/\Delta$ is the energy density for a domain of infinite size with dipolar density σ_i, as defined in Eq. (A9). $S_i=LD_i$ is the area of the stripe with dipolar density σ_i and $\mu^2\equiv(\sigma_1-\sigma_2)^2K_d$. The sum in the last expression in Eq. (2.2) accounts for the dipolar energy of the boundaries.

It is interesting and important to note that this boundary energy is equivalent to that of a system with molecular densities $\sigma_1'=\sigma_1-\sigma_2$ and $\sigma_2'=0$. Since we shall be interested in this work only in the boundary energy, it is instructive to use this equivalent system. We use this equivalent physical picture in the schematic drawings of the stripe phase and consider a system of condensed-phase stripes with molecular density σ_1' (shaded stripes) separated by vacuum stripes. [This physical picture is appropriate for surface fractions $\phi<\frac{1}{2}$. For surface fractions $\phi>\frac{1}{2}$ one should interchange the indices $(1\leftrightarrow2)$.]

Using the approach of Flament and Gallet [23] (see Appendix A) we transform the surface integrals of Eq. (2.2) into line integrals over the boundaries of the stripes and obtain a physical picture of interacting boundaries. Using Eqs. (A13)–(A15) the electrostatic energy per cell in Eq. (2.2) may be rewritten as

$$E_{cell}=LD[\phi\epsilon_1+(1-\phi)\epsilon_2]-2L\mu^2\left[\ln\frac{D}{\Delta}+1+\ln\frac{\sin(\pi\phi)}{\pi}\right]. \tag{2.3}$$

We now introduce the microscopic (short-ranged) attractions through the line tension γ, which in principle may be calculated using a microscopic model. The difference between the free energy density of the stripe phase and that of a system with two homogeneous phases (i.e., two separate and infinite domains) with dipolar densities σ_1 and σ_2 and with the same volume fraction ϕ is given by

$$\Delta f=-\frac{2\mu^2}{D}\left[\ln\frac{D}{\Delta}+1+\ln\frac{\sin(\pi\phi)}{\pi}-\frac{\gamma}{\mu^2}\right]. \tag{2.4}$$

This energy difference arises only from the energy of the boundaries in the system (including boundary-boundary interactions). Minimizing Δf with respect to D gives the equilibrium period of the supercrystal,

$$D=\frac{\pi\Delta}{\sin(\pi\phi)}e^{\gamma/\mu^2}, \tag{2.5a}$$

and the stripe width, D_1, is given by

$$D_1=\phi D=\frac{\Delta}{\mathrm{sinc}(\pi\phi)}e^{\gamma/\mu^2}, \tag{2.5b}$$

where $\mathrm{sinc}(x)\equiv\sin(x)/x$. [These quantities differ from those obtained by McConnell *et al.* [16] by a factor e that arises from the multipole correction term in Eq. (A14). In order to obtain the correct result in their work one should replace the line tension λ by $\lambda-\mu^2$.] Using Eq. (2.5a) in Eq. (2.4) we obtain $\Delta f=-2\mu^2/D<0$ and thus the energy of the stripe phase is always lower than that of a system with two homogeneous phases.

We note some interesting physical properties of the system as given by these equilibrium quantities. The dependence of the stripe width, D_1, on the area fraction ϕ is very weak for $\phi\lesssim\frac{1}{2}$. Defining the stripe width at $\phi=0$ as

$$D_0\equiv\lim_{\phi\to0}D_1=\Delta e^{\gamma/\mu^2}, \tag{2.6}$$

we find that the width of the stripes is relatively fixed, changing from $D_1=D_0$ at $\phi=0$ to $D_1\approx1.6D_0$ at $\phi=\frac{1}{2}$. Thus, the system responds to a change in the surface fraction by adjusting the period of the supercrystal rather than the width of the stripes. By rewriting Eq. (2.4),

$$\Delta f=-\frac{2\mu^2}{D}\left[\ln\frac{D_1 e}{\Delta}+\ln[\mathrm{sinc}(\pi\phi)]-\frac{\gamma}{\mu^2}\right], \tag{2.7}$$

it is possible to distinguish between the first term (E_s), which accounts for the self-energy of the stripe and the second one (E_{int}), which accounts for the interstripe interactions. In the regime $\phi \lesssim \frac{1}{2}$ these energies satisfy $E_{int}/E_s \ll 1$; thus, a change in D_1 is energetically very costly compared with a change in the period $D = D_1/\phi$. This stability will be demonstrated more explicitly in the treatment of the antisymmetric fluctuations of the boundaries in Sec. IV. Note that the dependence of the period D on the surface fraction ϕ is symmetric with respect to $\phi = \frac{1}{2}$. This symmetry is a property of Δf as seen in Eq. (2.4). As a consequence, if one considers the regime $\phi \geq \frac{1}{2}$ all the previous discussion is applicable with the replacements $D_1 \rightarrow D_2$ and $\phi \rightarrow (1-\phi)$.

It is interesting to note that the effect of the equilibrium interstripe interactions [second term in the parenthesis in Eq. (2.7)] is merely to increase the bare microscopic line tension γ. However, as we discuss in the following sections, the effective line tension for the symmetric modes of this phase is zero and due to the long-range dipolar interactions there exists no trivial (microscopic) line tension for the antisymmetric modes.

III. THE SYMMETRIC FLUCTUATION MODES OF THE STRIPES

In Appendix C we analyze the normal mode spectrum of the stripe phase in the harmonic approximation, and show that it contains both optical and acoustic branches. However, if one considers only long-wavelength modes, which dominate some of the physical properties of the system, one finds that the acoustic modes coincide with the symmetric modes of the stripes; this leads to a simplified physical picture of the fluctuating stripe phase.

In this section we show that the symmetric fluctuation modes of the stripes can have large amplitudes. This results in a failure of our second-order (harmonic) approximation for the fluctuation Hamiltonian at large length scales. However, we find that the harmonic approximation of the Hamiltonian *is* appropriate to describe the orientational order of the stripe phase. We consider the normal to the stripe boundary $\hat{\tilde{n}}(x)$ and calculate the normal-normal correlation function, $g_n(x) = \langle |\hat{\tilde{n}}(x) - \hat{\tilde{n}}(0)|^2 \rangle$. We find that normals to the boundary of the same stripe are highly correlated at all length scales. This result implies that the stripe phase exhibits long-range orientational order and that the smectic structure persists over large length scales. We stress that in order to obtain the full physical picture one should go to higher orders [20] in the fluctuation amplitude; however, we expect according to our result that the orientational order of the phase is long ranged in the more detailed theory as well.

It has been shown by other authors [15,20] that, in such two-dimensional systems, free dislocations are present at any finite temperature. The finite dislocation density, n_D, results in blobs of area ξ_D^2, which are free of dislocations. Combining this result with the one we obtain implies that within the blobs the smectic structure persists. This physical picture may fail, however, when the size of the blobs becomes small compared with the stripe periodicity, D, since then one can no longer refer to a supercrystal structure. Our result also implies that the dislocations, rather than the boundary fluctuations of the stripes, lead to the destruction of the supercrystal phase at higher temperatures.

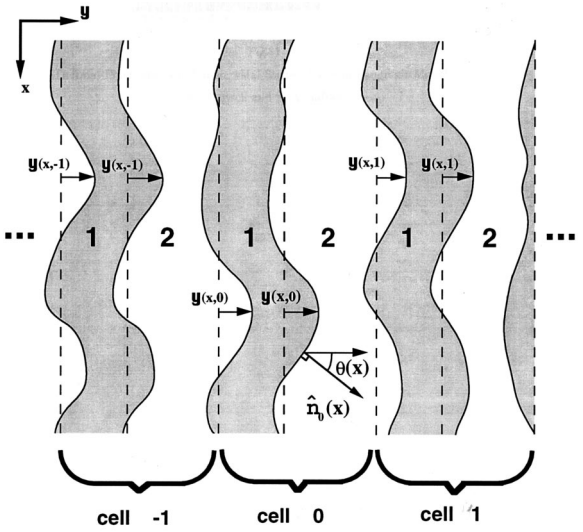

FIG. 2. The symmetric modes of the stripe phase. The equilibrium positions of the stripe boundaries are shown in dashed lines. Each boundary fluctuates with an amplitude $y(x,i)$, where i is the cell index. Thus, the stripe width does not change from its equilibrium value, and there is only one degree of freedom per cell. The figure shows $\hat{\mathbf{n}}_0(x)$, which is the normal to the boundary of the stripe (labeled 1) in the zeroth cell at the point $(x,y(x))$. The angle that this normal makes with the $\hat{\mathbf{y}}$ axis is denoted $\theta(x)$.

We use an approximation that treats the symmetric and antisymmetric modes of the stripes independently. At the end of Appendix C we argue that this approximation is justified for long-wavelength modes in the $\hat{y}$ direction. In this section we show that for the symmetric modes, the long-wavelength modes are energetically less costly and hence have the largest amplitudes. In Sec. IV we show that the antisymmetric modes result in a relatively large restoring force. Therefore, these modes are energetically unfavorable and their amplitude is much smaller than that of the symmetric modes. We thus neglect the coupling between the symmetric and antisymmetric modes, and use a simplified model for the analysis of the symmetric modes. This model, as shown in Fig. 2, takes the width of the stripes (labeled 1) to be constant, but allows them to fluctuate with amplitudes $y(x,i)$, where i is the cell index [i.e., $y_1(x,i) = y_2(x,i) \equiv y(x,i)$, using the notation of Appendix C, see also Fig. 6]. Experimental data (see, for example, Ref. [24]) indicate that the stripe width is relatively constant and hence agree qualitatively with this model. This description is appropriate only for surface fractions less than $\frac{1}{2}$, since at $\phi = \frac{1}{2}$ the interaction between two boundaries of adjacent stripes has the same weight as the one between the two boundaries of the same stripe. Thus, for $\phi \gtrsim \frac{1}{2}$ the two types of domains (1,2) interchange their roles and one should fix the width of the stripes labeled 2 in order to get the same results. With this model, which contains only symmetric modes, we have only one degree of freedom per cell, and Eq. (C4) for the full fluctuation Hamiltonian then reduces to

$$\Delta H_s = \frac{1}{2} \sum_{q,Q} |\tilde{y}(q,Q)|^2 \tilde{G}(q,Q), \tag{3.1}$$

where using Eq. (C3) $\tilde{y}(q,Q)$ is the discrete Fourier transform of $y(q,i)$, and $Q \in (-\pi/D, \pi/D)$ lies in the first Brillouin zone of the reciprocal lattice of the supercrystal. In Appendix F we calculate $\tilde{G}(q,Q)$ and find in the long-wavelength approximation (i.e., $qD, QD \ll 1$),

$$\tilde{G}(q,Q) \cong \frac{\mu^2}{D^2}[B_0(\phi)(QD)^2 + K_0(\phi)(qD)^4], \quad (3.2)$$

where $B_0(\phi)$ and $K_0(\phi)$, the dimensionless compression and bending moduli, respectively, are functions of the surface fraction ϕ. The compression and bending moduli of the system are related to these dimensionless quantities by the relations $B = (\mu^2/D) B_0$ and $K = \mu^2 D K_0$. This form of the Hamiltonian, ΔH_s, is in agreement with the elastic Hamiltonian used for lamellar phases and the system in equilibrium has no effective line tension as a consequence of its spatial isotropy (see, for example, Ref. [13]). In Appendixes F and G we explicitly show the vanishing of the effective line tension [i.e., the vanishing of the coefficient of the $(qD)^2$ term]. Such an elastic Hamiltonian was derived phenomenologically both in the vicinity of the critical point [13] of this phase, where the variation of the dipolar moment density in the $\hat{y}$ direction is small, and at low temperatures [14], where domain walls are sharp. It was calculated exactly for the acoustic modes in similar systems of ultrathin magnetic films [19]. We independently calculated it for the symmetric modes, offering a simple physical picture of the stripes with analytic expressions for the elastic constants for an arbitrary surface fraction.

It is interesting to note that the elastic approximation is valid when both $(qD) \ll 1$ and $(QD) \ll 1$. Hence, the period of the supercrystal, D, has the same role in this sense in both the $\hat{x}$ and the $\hat{y}$ directions. Specifically, we find (in the limit $\Delta/D \to 0$)

$$K_0(\phi) = \frac{1}{4\pi^2} \sum_{k=1}^{+\infty} \frac{\sin^2(\pi k \phi)}{k^3}, \quad (3.3a)$$

$$B_0(\phi) = 2[1 + \mathrm{sinc}^{-2}(\pi\phi) - 2(\pi\phi)\cot(\pi\phi)]. \quad (3.3b)$$

The result for B_0 can be derived alternatively [17,25] using the equilibrium free energy density of Eq. (2.4),

$$B_0 \equiv \frac{D^2}{\mu^2} \frac{\partial^2(\Delta f D)}{\partial D^2}. \quad (3.4)$$

Using the fluctuation Hamiltonian we now quantify the amount of disorder in the stripe structure due to thermal fluctuations. A convenient and conventional quantity describing the order of the stripes is the director, or the normal to the stripe boundary (see, for example, Ref. [26]). Due to the symmetry of the supercrystal the directors of different stripes obey the same statistics, and we choose to do the calculations for the stripe labeled zero. We introduce the normal-normal correlation function,

$$g_n(x) = \langle |\hat{\hat{n}}_0(x) - \hat{\hat{n}}_0(0)|^2 \rangle = 2(1 - \langle \cos[\theta(x) - \theta(0)] \rangle), \quad (3.5)$$

where $\theta(x)$, as shown in Fig. 2, is the angle between $\hat{\hat{n}}_0(x)$ and $\hat{\hat{y}}$ [i.e., $\theta(x) \equiv 0$ in equilibrium]. For small deviations of the normal from its equilibrium value we use the Gaussian approximation for the fluctuation Hamiltonian, Eq. (3.1), and the normal-normal correlation function is rewritten

$$g_n(x) = 2(1 - e^{-(1/2) g_\theta(x)}), \quad (3.6)$$

where $g_\theta(x) \equiv \langle |\theta(x) - \theta(0)|^2 \rangle$ is the angle correlation function. Using Eq. (3.2) in the equipartition relation $\langle |\tilde{y}(q,Q)|^2 \rangle = T/\tilde{G}(q,Q)$ we find

$$\begin{aligned} g_\theta(x) &\equiv \langle |\theta(x) - \theta(0)|^2 \rangle = \frac{2}{L} \sum_q q^2 \langle |y(q,0)|^2 \rangle [1 - \cos(qx)] \\ &= \frac{2T}{NL} \sum_{q,Q} \frac{q^2[1 - \cos(qx)]}{\tilde{G}(q,Q)} \\ &= \frac{DT}{2\pi^2} \int_{-\pi/D}^{+\pi/D} dQ \int_{-\infty}^{+\infty} dq \frac{q^2[1 - \cos(qx)]}{\tilde{G}(q,Q)} \\ &= \frac{2T\chi(\phi)}{\pi D \mu^2 \sqrt{B_0 K_0}} (1 - e^{-|x/\xi_c|} \mathrm{sinc}(|x/\xi_c|)) \\ &= \frac{T}{K\chi(\phi)} (1 - e^{-|x/\xi_c|} \mathrm{sinc}(|x/\xi_c|)), \end{aligned} \quad (3.7)$$

where $\xi_c = D/\chi(\phi)$ is the correlation length of the normal and $K = \mu^2 D K_0$ is the bending modulus of the system. $\chi(\phi) = \sqrt{\pi/2}(B_0/K_0)^{1/4}$ is a dimensionless, slowly varying function of ϕ of the order of unity. We are interested in the large scale behavior of the system. In the limit $x \to \infty$ the angle correlation function approaches a finite value, which is independent of x, but is a function of the surface fraction

$$g_c(\phi) = \lim_{x \to \infty} g_\theta(x) = \frac{T}{K\chi(\phi)} \equiv \frac{\sin(\pi\phi)}{\pi K_0(\phi)\chi(\phi)} \frac{T}{\mu^2 \Delta} e^{-b_N}, \quad (3.8)$$

where the ratio $b_N \equiv N_B^{-1} = \gamma/\mu^2$ (N_B is generally referred to as the *bond number*). In Fig. 3 we plot $g_c(\phi)$ in units of the dimensionless parameter $(T/\mu^2\Delta)e^{-b_N}$. Our continuum model is valid [see Eqs. (2.5)] for $e^{b_N} \gg 1$ and hence $e^{-b_N} \ll 1$. Thus, $(T/\mu^2\Delta)e^{-b_N}$ is generally exponentially small and we find that $g_c \ll 1$ for all realistic surface fractions (i.e., $\phi \gg e^{-b_N}$) [10]. [$T/\mu^2\Delta = (T/\gamma\Delta) b_N$ and $T/\gamma\Delta \sim 1$ in the vicinity of the critical point. Thus, at room temperatures we estimate that $T/\mu^2\Delta \sim 1$ and in any case not much greater than 1.] Using the definition, Eq. (3.6), this implies that the normal does not decorrelate at large length scales,

$$\lim_{x \to \infty} \langle |\hat{n}_0(x) - \hat{n}_0(0)|^2 \rangle = \lim_{x \to \infty} 2(1 - e^{-(1/2) g_\theta(x)}) \cong g_c(\phi) \ll 1, \quad (3.9)$$

orientational order is maintained, and our Gaussian (harmonic) approximation is valid for the director field. However, as already mentioned by other authors [19] (for the case $\phi = \frac{1}{2}$), we find that the mean square fluctuations of a stripe

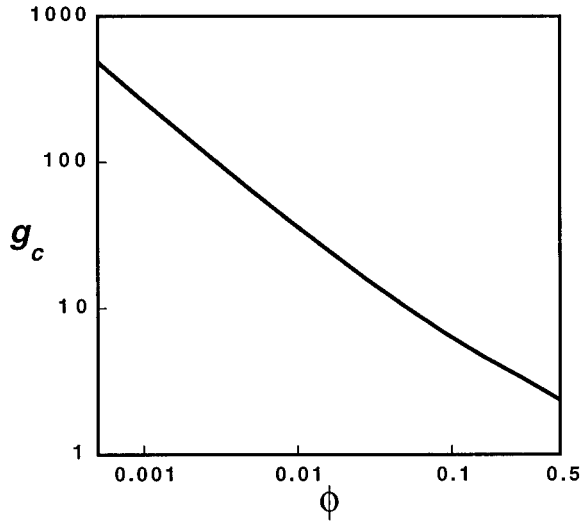

FIG. 3. The limit of the correlation function of the angle of the normal, $g_c(\phi)$, at large length scales (i.e., $x \gg \xi_c$) in units of the dimensionless parameter $(T/\mu^2\Delta)e^{-b_N}$, which is generally exponentially small. Thus, for realistic values of the surface fraction (i.e., $\phi > e^{-b_N}$) we find that $g_c(\phi) \ll 1$ and the angle does not decorrelate.

$\langle |y(x,i)|^2 \rangle$ diverge in the thermodynamic limit for any surface fraction ϕ, and hence the stripe phase loses its compressional rigidity. This divergence is overcome by the natural finite size cutoff that exists in the system due to the finite density of free dislocations. The dislocations will result in asymmetric blobs of area ξ_D^2 in which the stripe order will persist [15,20]. The long-range order of the normal suggests that finite stripes (due to dislocations) will be relatively straight as long as the stripe supercrystal order is still present locally.

It is interesting to find the condition for the validity of this physical picture. The dislocation density is $n_D \approx a_c^{-2} \exp(-E_D/k_B T)$, where a_c is the dislocation core diameter and E_D is the isolated edge dislocation energy. Far from the critical point E_D is of the order of the bending modulus K [27]. Numerical evaluation of K leads to a rough estimate that even at room temperatures the dislocation length scale ξ_D will become comparable with the stripe periodicity D only at surface fraction as low as $\phi \approx 0.1$ (the lower bound for the surface fraction is increasing with temperature). Thus our physical picture is valid for a wide range of surface fractions and temperatures.

Our analysis fails when the amount of disorder is increased (e.g., higher temperatures), leading to isotropic phases. However, it is striking that even in what seems in experiments like isotropic phases [3,24], the stripes tend to maintain their width and their symmetric modes are dominant.

IV. ROUGHNESS OF THE STRIPE BOUNDARY

We now extend the calculation of Sec. III to include fluctuations in the stripe width (i.e., antisymmetric modes of the boundaries). These fluctuations are important both for liquid and solid stripes. In the case of a surface of a solid, the mean square of the fluctuations determines whether the surface is rough or faceted. In a liquid/gas interface the dynamics of these fluctuations is important for the behavior of capillary waves. Using a mean field approximation we find two scaling regimes for the mean square fluctuations of the stripe width $y_0(x)$: (a) the high-temperature regime, where $\langle y_0^2 \rangle \sim D_1 \Delta$ and (b) the low-temperature regime, where $\langle y_0^2 \rangle \sim \Delta^2$. The appropriate scaling regime is determined by the dimensionless parameter $\sim T/\mu^2\Delta$. In regime (b) we find for the solid stripe case that the long-range dipolar interactions may induce faceting in the stripe boundaries via a first-order phase transition. [The transition is in fact between an almost rough interface and a faceted one, as explained after Eq. (4.13).]

A. Stripe-width fluctuations

Previously, we considered the symmetric modes alone and froze one of the two degrees of freedom that exist per cell by fixing the widths of the stripes to their equilibrium values. In this section we demonstrate that this physical picture is realistic, due to the fact that the stripe-width fluctuations are very small on the scale of the stripe width. We use an approximation that treats the symmetric and antisymmetric modes of the stripes independently. At the end of Appendix C we argue that this approximation is justified for long-wavelength modes in the $\hat{y}$ direction. In the case of the symmetric modes, the long-wavelength modes are energetically less costly and hence have the largest amplitudes. Thus, for calculations of physical quantities that depend mainly on the symmetric fluctuations it is justified to neglect the coupling between the symmetric and antisymmetric modes. In this section we investigate the statistics of the width fluctuations of the stripes (i.e., antisymmetric modes). For these fluctuations it is harder to justify such separation between the symmetric and the antisymmetric modes. In order to do that one has to go to the full fluctuation Hamiltonian in Eqs. (C4) and (C5), transform the vector $\tilde{Y}(q,Q)$ into symmetric and antisymmetric components, and compare the magnitude of the cross terms to that of the diagonal ones. Such a calculation is intractable analytically and its numerical evaluation is left to future work. However, we assume that in order to find the qualitative behavior of the width fluctuations it is sufficient to consider the antisymmetric modes independently and we use a simplified model to describe the system.

In Sec. III we found that the stripes can be considered as locally straight and that the symmetric modes that have large amplitudes are the long-wavelength ones. Thus, when considering the antisymmetric modes we use a model that contains no symmetric modes. This model is consistent with our result that the antisymmetric modes that have the largest amplitudes are those with wavelengths comparable with the stripe width. In addition, we note that the terms that dominate the fluctuation energy are those which arise from the self-energies of the stripes. We also assume that statistically (at high enough temperatures), the antisymmetric modes of different stripes are not coherent.

Hence, it is appealing to use a mean field approximation and to consider the antisymmetric modes only for one of the stripes (labeled zero). Thus, in our simplified model the stripe boundaries fluctuate only with antisymmetric modes and all the other stripes are at their equilibrium

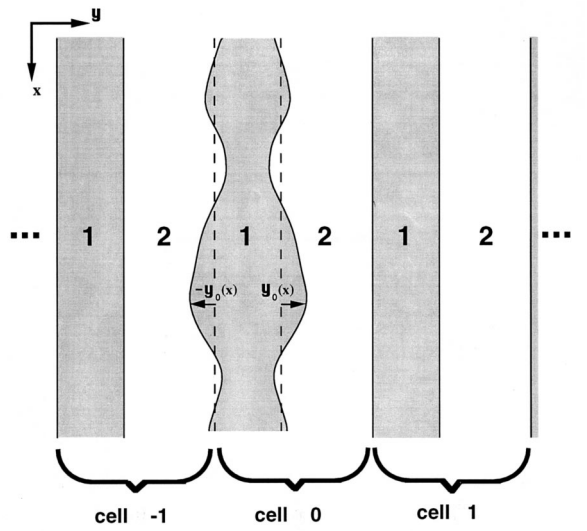

FIG. 4. The antisymmetric modes of the stripe labeled 1 in the zeroth cell (the choice of the stripe is irrelevant due to the symmetry of the phase). The boundaries of the stripe fluctuate with amplitudes $y_0(x)$ and $-y_0(x)$. We use a mean field approximation, where the rest of the cells are in their equilibrium state.

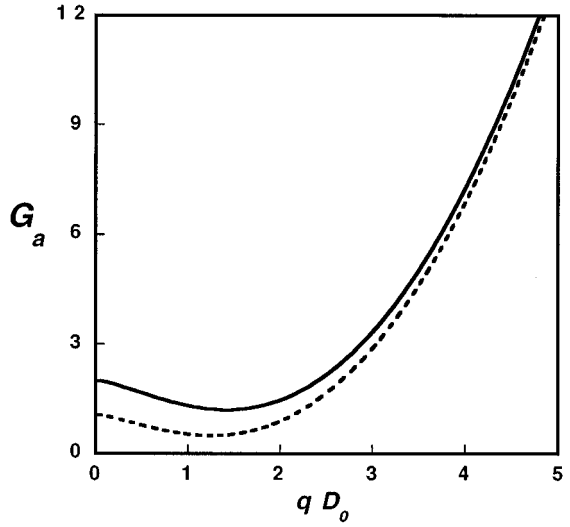

FIG. 5. The kernel of the antisymmetric modes $G_a(q)$ in units of $4\mu^2/D_0^2$ as a function of the dimensionless wave number qD_0. The solid curve corresponds to $\phi=0$ and the dashed curve corresponds to $\phi=\frac{1}{2}$.

state, as sketched in Fig. 4. This implies (using the notation of Appendix C) $y_1(x,0)=-y_2(x,0)\equiv y_0(x)$ and $y_m(x,i)\equiv 0$ for $i\neq 0$. Equation (C4) for the fluctuation energy then reduces to

$$\Delta H_a=\frac{1}{2}\sum_q |y_0(q)|^2 G_a(q). \tag{4.1}$$

The detailed derivation of $G_a(q)$ is given in Appendix H,

$$G_a(q)=4\mu^2\left\{D_0^{-2}[1-\tfrac{1}{3}\sin^2(\pi\phi)]+q^2\left[\frac{K_1(q\Delta)}{q\Delta}-\frac{1}{(q\Delta)^2}+\frac{K_1(qD_1)}{qD_1}+\frac{1}{2}\frac{\gamma}{\mu^2}\right]\right\}, \tag{4.2}$$

where $K_1(x)$ is the modified Bessel function of order 1 and $D_0=\Delta e^{\gamma/\mu^2}$ is given by Eq. (2.6). Expanding $G_a(q)$ for $q\ll q_{max}\sim 1/\Delta$ we obtain

$$\begin{aligned}G_a(q)&\cong 4\mu^2\left\{D_0^{-2}[1-\tfrac{1}{3}\sin^2(\pi\phi)]+q^2\left[\tfrac{1}{2}(\ln|q\Delta|-\beta)+\frac{K_1(qD_1)}{qD_1}+\frac{1}{2}\frac{\gamma}{\mu^2}\right]\right\}\\&=\frac{4\mu^2}{D_0^2}\{\alpha(\phi)+(qD_0)^2[\ln|qD_0|-\beta-\tfrac{1}{2}\ln[\mathrm{sinc}(\pi\phi)]+M(qD_1)]\},\end{aligned} \tag{4.3}$$

where in the last step we used the equilibrium value of D_1, given by Eq. (2.5b); $\beta=\ln 2+\frac{1}{2}-\gamma_E>0$ and $\gamma_E=0.577\,216$ is the Euler constant. $M(x)$ is a function which is significant only for large values of qD_1,

$$M(x)=\frac{K_1(x)}{x}-\frac{1}{x^2}-\tfrac{1}{2}(\ln|x|-\beta);\quad \lim_{x\to 0}M(x)=0. \tag{4.4}$$

The effect of the other stripes enters through $\alpha(\phi)$, which is a positive and slowly varying function of ϕ,

$$\alpha(\phi)=1+\sin^2(\pi\phi)[(\pi\phi)^{-2}-\tfrac{1}{3}];\qquad \lim_{\phi\to 0}\alpha(\phi)=2;\quad \alpha(\tfrac{1}{2})\approx 1.1. \tag{4.5}$$

Thus, in this mean field approximation the total effect of the other stripes is to *decrease* the restoring force on variations from the equilibrium stripe width, D_1. This result may seem surprising, since the interstripe interactions tend to *increase* the restoring force with increasing surface fraction ϕ, due to the decreasing distance between the stripes. However, the stripe width D_1 increases with increasing ϕ. Thus, the stripe self-interaction energy (i.e., interactions between the stripe boundaries) decreases as ϕ increases. This dominates in the total restoring force, which decreases with increasing ϕ. [Note that this discussion and the following analysis are relevant only for $\phi\lesssim\frac{1}{2}$. For $\phi>\frac{1}{2}$ the roles of the domains interchange (i.e., $1\leftrightarrow 2$).] This result is in complete agreement with the discussion of the energy scales in equilibrium at the end of Sec. II.

$G_a(q)$ is plotted in Fig. 5 for the two extreme surface fractions, $\phi=0$ and $\phi=\frac{1}{2}$. It shows that the surface fraction has little qualitative effect on the energy spectrum. The existence of a minimum for $G_a(q)$ implies that fluctuations of the stripe width will be largest at this wavelength, whose value is on the order of the stripe width D_1. This suggests that the transition from the stripe phase to the bubble phase will be to bubbles with diameters of the order of the stripe width. The fact that this characteristic length scale is indeed much smaller than those of the symmetric modes supports our assumption at the beginning of this section.

Using Eq. (4.4) in the limit $qD_1 \ll 1$, $G_a(q)$ is further simplified,

$$G_a(q) \cong \frac{4\mu^2}{D_0^2}(\alpha(\phi) + (qD_0)^2\{\ln|qD_0| - \beta - \tfrac{1}{2}\ln[\mathrm{sinc}(\pi\phi)]\}). \quad (4.6)$$

This approximate form implies that $G_a(q)$ has essentially a quadratic dependence on (qD_0) at low values of this argument. We thus phenomenologically approximate $G_a(q)$ by a parabola

$$G_{ap}(q) = a\mu^2[(|q|-c)^2 + b^2], \quad (4.7)$$

where $a, b,$ and c are functions of ϕ, that are obtained by fitting $G_{ap}(q)$ of Eq. (4.7) to $G_a(q)$ of Eq. (4.3). In principle we find that $a \sim 1$ and $b, c \sim 1/D_1$.

Using Eq. (4.7) and the equipartition relation $\langle |y_0(q)|^2 \rangle = T/G_{ap}(q)$ we calculate the mean square fluctuation of the stripe boundary,

$$\langle y_0^2 \rangle = \frac{1}{L}\sum_q \langle |y_0(q)|^2 \rangle \cong \frac{1}{\pi}\int_0^\infty dq \frac{T}{G_{ap}(q)} = \frac{T}{\pi a b \mu^2}\left[\arctan\left(\frac{c}{b}\right) + \frac{\pi}{2}\right] \approx \frac{1}{4}\frac{T}{\mu^2\Delta} D_1\Delta, \quad (4.8)$$

where L is the length of the stripes. This scaling is obtained for both extreme values of the surface fraction, $\phi = 0$ and $\phi = \frac{1}{2}$. We find it to be in good agreement with an exact numerical evaluation of $\langle y_0^2 \rangle$ using $G_a(q)$ of Eq. (4.3). It is interesting to note that by adjusting $T/\mu^2\Delta$ we obtain two scaling regimes for the amplitude of the mean square fluctuation of the boundary (note, however, that the relation $e^{\gamma/\mu^2} \gg 1$ must hold for consistency): (a) if $T/\mu^2\Delta \sim 1$, then $\langle y_0^2 \rangle \sim D_1\Delta$; (b) if $T/\mu^2\Delta \sim e^{-\gamma/\mu^2}$, then $\langle y_0^2 \rangle \sim \Delta^2$. Both regimes obey $\langle y_0^2 \rangle \ll D_1^2$, which means that the fluctuations of the stripe width are very small on the scale of the stripe width. This result supports our model in Sec. III, where we fixed the stripe width to its equilibrium value. The qualitative difference between the two regimes is manifested in the context of the analysis of the roughness of a solid stripe (i.e., a stripe that consists of a crystalline monolayer).

B. Roughening of solid stripes

The stripe phase that we now focus on consists of crystalline domains separated by dilute gas domains. This phase is characterized by an additional restoring force on its interface position, due to the crystal periodic potential, which tends to pin the interface. While the minimization of the energy of the system results in a periodic striped structure (faceted phase), the entropy associated with the wandering of the interfaces between these stripes tends to delocalize the nominally straight domain wall boundaries (rough phase). The following analysis is for one interface, but the result is relevant for any of the stripe boundaries of the supercrystal. We emphasize that our calculations are within the framework of a mean field approximation that decouples the symmetric fluctuation modes from the width fluctuations. Therefore, our results relate to ''local'' roughness and faceting, since the symmetric fluctuation modes do have divergent amplitudes at large enough scales so that the crystal is not well defined at very large length scales due to the symmetric modes.

Using the notations of Ref. [23], we consider a one-dimensional interface with equilibrium position parallel to the $\hat{x}$ direction. The pinning effect can be modeled by a periodic potential $U(y)$, where $\hat{y}$ is the direction normal to the interface. For a given interface deformation $y_0(x)$, the interface pinning energy E_p is written

$$E_p = \int_{-L/2}^{L/2} dx U(y_0(x)). \quad (4.9)$$

The interface state is determined by the average of the pinning energy, $\langle E_p \rangle$, over the fluctuations. If $\langle E_p \rangle / L$ is finite as the interface length L goes to infinity, the interface is smooth (nondiverging) and U is relevant on large scales. However, if $\langle E_p \rangle / L$ goes to zero in this limit, the long-wavelength fluctuations are identical to those in the liquid state. In this case, U is not relevant on large scales and the interface is rough. In its general form, $\langle E_p \rangle$ is written

$$\langle E_p \rangle = \int\int dx\ \mathcal{D}[y_0(x)] U(y_0(x)) P[y_0(x)], \quad (4.10)$$

where $P[y_0(x)] \sim \exp\{-\Delta H_p[y_0(x)]/T\}$ is the probability for a thermal fluctuation to have a configuration $y_0(x)$ and the integration $\int \mathcal{D}[y_0(x)]$ is performed over all possible configurations of $y_0(x)$. Using Eqs. (4.1) and (4.9) the fluctuation Hamiltonian that includes the pinning energy is written

$$\Delta H_p[y_0(x)] = \Delta H_a[y_0(x)] + E_p[y_0(x)]. \quad (4.11)$$

However, using this form of ΔH_p is generally intractable even for the simplest forms of the pinning potential $U(y)$. Thus, we shall investigate the system using approximate approaches. In what follows we describe two such approaches. The first one treats $U(y)$ as a small perturbation and the second one is less restricted and uses a self-consistent variational approach. In both approaches we use harmonic approximations for ΔH_p, which are thus tractable.

1. Perturbation calculation

Calculations in three dimensions have shown [28] that the interface state does not depend on the details of U and that a roughening transition temperature (T_R) always exists. A similar calculation for a two-dimensional system shows that for the case of short-range interactions $T_R \equiv 0$. In our analysis, we examine the effect of the long-range interactions on the interface state.

For simplicity we take $U(y) = -U_0\cos(2\pi y/\Delta_0)$, where $\Delta_0 \sim \Delta$ is the crystal period (of the internal crystalline structure of the stripe) in the $\hat{y}$ direction. Using this potential in a system which is modeled by a harmonic Hamiltonian, $\langle E_p \rangle_h$ is written

$$\langle E_p\rangle_h = -\int\int dx\ \mathcal{D}[y_0(x)]U_0\cos\left(2\pi\frac{y_0(x)}{\Delta_0}\right)P_h[y_0(x)]$$
$$= -U_0L\ \exp\left[-2\pi^2\frac{\langle y_0^2\rangle_h}{\Delta_0^2}\right], \tag{4.12}$$

where the subscript h is used to denote that the averaging is done with respect to the harmonic Hamiltonian.

Using the first approach we now treat $U(y)$ as a small perturbation. Noting that ΔH_a is already harmonic, we can write $\Delta H_p \cong \Delta H_a$ and to first order in U we find

$$\langle E_p\rangle \cong -U_0L\ \exp\left[-2\pi^2\frac{\langle y_0^2\rangle}{\Delta_0^2}\right], \tag{4.13}$$

where $\langle y_0^2\rangle$ is given by Eq. (4.8).

It is interesting to note how the two scaling regimes that were found for $\langle y_0^2\rangle$ affect the roughness of the interface. In regime (a), where $T/\mu^2\Delta \sim 1$ and $\langle y_0^2\rangle \sim D_1\Delta$, the absolute value of the argument of the exponent in Eq. (4.13) is exponentially large ($\sim e^{\gamma/\mu^2}$), but does not diverge in the thermodynamic limit. This result is unique in the sense that it does not correspond to the classical case of a rough interface, where the argument of the exponent diverges in the thermodynamic limit, resulting in $\langle E_p\rangle = 0$. However, since the restoring potential is exponentially small, it is not sufficient to make the interface smooth on the microscopic scale and the interface is for practical purposes quite rough in this regime [e.g., the correlation length of the interface fluctuations is exponentially large, as shown using the second approach in Eq. (4.26)]. At very small values of $T/\mu^2\Delta \sim e^{-\gamma/\mu^2}$, we enter scaling regime (b), where $\langle y_0^2\rangle \sim \Delta^2$. In this regime, the argument of the exponent may become of the order of unity, resulting in a faceted (nonrough) interface.

In realistic Langmuir monolayers it seems that the parameters cannot reach the extreme values needed for the second scaling regime and thus we do not expect faceting according to this approximation approach. Still, the roughness of the interface can be reduced drastically to be somewhere between the two regimes. However, these calculations are valid for any two-dimensional system with dipolar interactions and there may be other systems (e.g., ultrathin ferromagnetic layers) for which the parameters may fall within the second scaling regime, and thus induce faceting.

2. Self-consistent theory

We now extend our analysis and use the second approach, which treats self-consistently the effect of the pinning potential in the fluctuation Hamiltonian. Using this approach we show that the roughening transition is in fact less restricted than what is predicted by the perturbative approach and that the transition may be a first-order one.

We follow Ref. [29] and investigate the system using an approximate variational approach. We consider a reference Hamiltonian $\mathcal{H}_r$, which is tractable, and use the theorem [30] that bounds the exact free energy, F_e, by

$$F_e < F = F_r + \langle \Delta H_p - \mathcal{H}_r\rangle_r, \tag{4.14}$$

where F_r is the free energy of a reference system and the subscript r denotes that the average is taken with respect to the Boltzman factor $e^{-\mathcal{H}_r/T}$ of the reference Hamiltonian. We use a harmonic approximation for the reference Hamiltonian, which is thus written

$$\mathcal{H}_r = \tfrac{1}{2}T\sum_q G(q)|y_0(q)|^2. \tag{4.15}$$

Using Eqs. (4.1), (4.11), and (4.12) and the equipartition relation $\langle |y_0(q)|^2\rangle_r = 1/G(q)$, Eq. (4.14) is rewritten

$$F = F_c + \frac{T}{2}\sum_q \ln G(q) + \frac{1}{2}\sum_q \frac{G_a(q)}{G(q)} - LU_0e^{-2\pi^2 g_0}, \tag{4.16}$$

where F_c is a constant and g_0 is defined as

$$g_0 = \frac{1}{L\Delta_0^2}\sum_q [G(q)]^{-1} \equiv \frac{\langle |y_0|^2\rangle_r}{\Delta_0^2}. \tag{4.17}$$

We now minimize F with respect to $G(q)$ and find the equation that defines $G(q)$

$$\frac{T}{G(q)} - \frac{G_a(q)}{G(q)^2} - \frac{4\pi^2U_0\Delta_0^{-2}}{G(q)^2}e^{-2\pi^2g_0} = 0. \tag{4.18}$$

We thus find

$$G(q)^{-1} = \frac{T}{G_a(q) + a\mu^2\xi^{-2}}, \tag{4.19}$$

where using Eq. (4.12) we find

$$\xi^{-2} = \frac{4\pi^2U_0}{a\mu^2\Delta_0^2}e^{-2\pi^2g_0} \equiv \frac{4\pi^2}{a\mu^2\Delta_0^2L}|\langle E_p\rangle_r|. \tag{4.20}$$

In the latter expression we explicitly observe the role of the intensive quantity $\langle E_p\rangle/L$. If it is finite in the thermodynamic limit, ξ^{-2} is finite and $G(q)$ differs from $G_a(q)$ (i.e., the pinning potential is relevant). However, if it vanishes we have $\xi^{-2} \to 0$, $G(q) \to G_a(q)$ and the pinning potential is not relevant.

Since g_0 is related to the sum over all the $G(q)$, Eq. (4.19) has to be solved self-consistently to yield a value for ξ. We use Eq. (4.7) to approximate $G_a(q)$ by $G_{ap}(q)$. Performing the sum over q in Eq. (4.19) we obtain g_0, which is then used in Eq. (4.20) to derive an equation for ξ. The result is

$$g_0=\frac{T}{\pi a\mu^2\Delta_0^2\sqrt{b^2+\xi^{-2}}}\left\{\arctan\left(\frac{c}{\sqrt{b^2+\xi^{-2}}}\right)+\arctan\left(\frac{\frac{\pi}{\Delta}-c}{\sqrt{b^2+\xi^{-2}}}\right)\right\}, \tag{4.21}$$

and

$$\left(\frac{\pi\xi}{\Delta_0}\right)^{-2}=\frac{4U_0}{a\mu^2}\exp\left\{-\frac{2\pi T}{a\mu^2\Delta_0^2\sqrt{b^2+\xi^{-2}}}\left[\arctan\left(\frac{c}{\sqrt{b^2+\xi^{-2}}}\right)+\arctan\left(\frac{\frac{\pi}{\Delta}-c}{\sqrt{b^2+\xi^{-2}}}\right)\right]\right\}. \tag{4.22}$$

Defining $\eta\equiv(\Delta_0/\pi\xi)^2$, the previous equation is rewritten

$$\eta=\alpha_0\exp\left\{-\frac{\tau}{\sqrt{\eta_0+\eta}}\left[\arctan\left(\frac{c_0}{\sqrt{\eta_0+\eta}}\right)+\arctan\left(\frac{\mathcal{R}-c_0}{\sqrt{\eta_0+\eta}}\right)\right]\right\}, \tag{4.23}$$

where we defined the following dimensionless parameters:

$$\alpha_0\equiv\frac{4U_0}{a\mu^2};\quad \tau\equiv\frac{2T}{a\mu^2\Delta_0};\quad \eta_0\equiv\left(\frac{b\Delta_0}{\pi}\right)^2;\quad c_0\equiv\frac{c\Delta_0}{\pi};$$

$$\mathcal{R}\equiv\frac{\Delta_0}{\Delta}\sim 1. \tag{4.24}$$

It is important to note that $\eta=0$ is not a solution to Eq. (4.23). It implies that as long as $\eta_0\neq 0$ $(b\neq 0)$, we have $\xi^{-2}\neq 0$ and thus $\langle E_p\rangle\neq 0$. The pinning potential is always relevant to some extent and as we concluded, using the first approach, the interface is never fully rough. Physically, the additional restoring force on the interface position due to the long-range interactions bounds the lowest free mode to be $q_{\min}\sim b\sim D_1^{-1}$, while for a free interface it is $\sim L^{-1}$ (system size limited). This effect is very strong for stripe domains, but we expect it to be irrelevant in systems of finite size domains, where the size cutoff is already related to the domain size and not to the system size.

In order to find whether faceting is possible in this system we have to explicitly solve Eq. (4.23) for $\eta(\xi)$. We find that at high temperatures there is only one solution $\xi_1\gg D_1$, which implies that the pinning effect is negligible. However, as the reduced temperature τ is decreased below a threshold value two new solutions $\Delta_0<\xi_{2,3}\ll D_1$ appear, where the solution with the smaller value of ξ, ξ_3, corresponds to a minimum of the free energy. As τ is further decreased, ξ_2 and ξ_1 vanish and ξ_3 thus corresponds to a global minimum of the free energy. This is a first-order transition mechanism and in order to quantify the transition we rewrite the free energy of Eq. (4.16) as a function of η and find its global minimum. Using the $G(q)$ that minimizes the free energy as given by Eq. (4.19), and using Eq. (4.7) to approximate $G_a(q)$ by $G_{ap}(q)$ we write the η dependent part of the free energy in a dimensionless form,

$$f(\eta)=\frac{2\Delta_0}{LT}F-f_c=c_0\ln(\eta+\eta_0+c_0^2)+(\mathcal{R}-c_0)\ln[\eta+\eta_0+(\mathcal{R}-c_0)^2]+\frac{2\eta_0+\eta}{\sqrt{\eta_0+\eta}}\left[\arctan\left(\frac{c_0}{\sqrt{\eta_0+\eta}}\right)+\arctan\left(\frac{\mathcal{R}-c_0}{\sqrt{\eta_0+\eta}}\right)\right]$$
$$-\frac{\alpha_0}{\tau}\exp\left\{-\frac{\tau}{\sqrt{\eta_0+\eta}}\left[\arctan\left(\frac{c_0}{\sqrt{\eta_0+\eta}}\right)+\arctan\left(\frac{\mathcal{R}-c_0}{\sqrt{\eta_0+\eta}}\right)\right]\right\}, \tag{4.25}$$

where all the η independent terms of the free energy F are lumped into f_c. Rewriting Eq. (4.23) with $\eta\ll\eta_0,c_0^2$ we find that above the transition temperature τ_R the value of the order parameter is

$$\eta_1\approx\alpha_0\exp\left\{-\frac{\tau}{\sqrt{\eta_0}}\left[\arctan\left(\frac{c_0}{\sqrt{\eta_0}}\right)+\frac{\pi}{2}\right]\right\}\ll\eta_0,c_0^2, \tag{4.26}$$

and we note that $\eta_0,c_0^2\sim e^{-2b_N}$, and thus η_1 is practically zero. Rewriting Eq. (4.23) with $\eta\gg\eta_0,c_0^2$ we find that below τ_R the value of the order parameter is determined by the self-consistent equation

$$\eta_3=\alpha_0\exp\left[-\frac{\tau}{\sqrt{\eta_3}}\arctan\left(\frac{\mathcal{R}}{\sqrt{\eta_3}}\right)\right]. \tag{4.27}$$

Below the transition temperature we expand $f(\eta)$ for $\eta\gg\eta_0,c_0^2$ and find the transition temperature by equating $f(\eta)=f(\eta_1)\approx 0$. Substituting $\mathcal{R}=1$ and using the limit $\alpha_0\ll 1$ in Eq. (4.27) we find that the transition is characterized by

$$\eta_R = \eta_3|_{\tau_R} \approx e^{-1}\alpha_0; \quad \tau_R \approx \sqrt{\frac{4\alpha_0}{\pi^2 e}}\, 0.386\sqrt{\alpha_0}. \tag{4.28}$$

This solution is thus restricted to strengths of pinning potential which fall in the range $\eta_0, c_0^2 \ll \alpha_0 \ll 1$. The upper limit is needed for our theory to be consistent, since $\alpha_0 \gtrsim 1$ implies $\xi_R \lesssim \Delta_0$ (i.e., the correlation length is shorter than the microscopic cutoff), which is not physical. Hence, for $\alpha_0 \gtrsim 1$ a more refined theory is needed in order to describe the system, but we still expect a first-order transition. For a very weak pinning potential ($\alpha_0 \lesssim \eta_0, c_0^2$) the first-order transition mechanism is destroyed and there is a smooth change in the correlation length ξ with temperature.

The predictions of the two different approaches may seem at first contradictory. The reason that the perturbative approach does not predict the first-order transition is that it only finds the solution ξ_1 and follows it as the temperature is decreased. Thus, this approach is correct at high enough temperatures, but fails in the low-temperature regime where the effect of the pinning potential is strong and hence it can be no longer treated perturbatively. The self-consistent approach indeed predicts that as the pinning potential becomes weaker (decreasing α_0) the roughening transition temperature is decreasing and therefore the perturbative approach becomes valid for lower temperatures. For very low values of $\alpha_0 \lesssim \eta_0, c_0^2$ the self-consistent approach does not predict a transition either. We conclude that the self-consistent approach is more general and that the perturbative approach is only a special case of it.

We note that the previous treatments of the roughening transition in two-dimensional systems (with only short-range interactions) predicted that it occurs only at $T_R \equiv 0$, due to the large fluctuations [31,32]. Our results suggest a possible first-order transition.

V. DISCUSSION

We now summarize our results and discuss their experimental implications. We emphasize that our predictions are relevant for the low-temperature regime, far enough from the critical point for the onset of the stripe order.

We calculated the equilibrium stripe width and stripe periodicity as functions of the surface fraction of the dense phase. The dependence of these quantities on the surface fraction is unique to systems with dipolar interactions. It is still unclear to what extent the real physical systems are indeed dominated by long-range dipolar interactions. Hence, measuring the surface fraction dependence of these quantities can verify this physical picture and will give an estimate of the *bond number* μ^2/γ.

In our analysis of the symmetric modes we found that the stripe phase exhibits long-range orientational order. We predicted that if the dislocation density is not too high, the stripes are practically straight within the blobs that are free of dislocations. This prediction can be qualitatively verified experimentally, probably by optical imaging. We assume that our infinite-length stripe model will have corrections due to the presence of dislocations, which will make the stripes less straight than our idealized model predicts.

In our analysis of the fluctuations in the stripe width we calculated the thermal roughness of the stripe boundaries. This quantity will enter into an analysis of the line shape in scattering from the stripes. In the case of solid stripes, our self-consistent calculation suggests a possible first-order roughening transition in a realistic region of the physical parameter space. This prediction has yet to be verified experimentally. We note that our treatment of this problem is within a framework of a mean field model. Thus, the effects of the distant stripes and the coupling to the symmetric fluctuation modes of the stripes may modify our results. Some more theoretical work that will include these effects as well as computer simulations based on a microscopic Hamiltonian of the interface must be done in order to complete the mean field picture that we have presented.

ACKNOWLEDGMENTS

We thank D. Andelman for his useful comments and for referring us to relevant work in this field. We are grateful to T. Lubensky for the enlightening discussion. We also acknowledge A. Cebers and D. Vanderbilt for communicating to us their papers, and V. Kaganer for his remarks. One of us (A.D.) would like to thank K. Gomberoff for useful discussions and important technical assistance. We are grateful for the support of the Israel Academy of Sciences and the Minerva Foundation, Munich, Germany.

APPENDIX A: SYSTEMS WITH LONG-RANGE POWER-LAW INTERACTIONS

In this Appendix we present a general formalism for the treatment of 2D systems with long-range power-law interactions. This formalism decouples the energy of the system into separate bulk and boundary terms. We then use this formalism in the specific case of dipolar interactions.

1. General case

We consider a 2D system of particles interacting through an isotropic repulsive pair potential (the attractive case was treated by Flament and Gallet [23]) which depends only on the interparticle distance

$$V_n = \frac{K_n}{R^n}, \tag{A1}$$

where $R = |\vec{r}_1 - \vec{r}_2|$ and with interaction strength $K_n > 0$. To describe phenomena on length scales much larger than those of a molecular size, it is appropriate to take the continuum limit, where we introduce the particle density $\sigma(\vec{r})$. The interaction energy between two domains S_1 and S_2 (which may overlap) can be written as

$$E_n = \frac{1}{2}\int_{S_1}\int_{S_2} d^2r_1 d^2r_2 \sigma(\vec{r}_1)\sigma(\vec{r}_2)V_n. \tag{A2}$$

In the following analysis we consider the case of homogeneous distributions of particles within each of the domains; in addition we assume that the system is at sufficiently low temperatures so that the domain boundaries are sharp. Hence, it is possible to write $\sigma(\vec{r}_1)\sigma(\vec{r}_2) \equiv \sigma_1\sigma_2$ for $R \geq a$ and

$\sigma(\vec{r}_1)\sigma(\vec{r}_2)\equiv 0$ for $R<a$, where a is the microscopic cutoff comparable to the interparticle spacing. Thus, the only spatial dependence in the integrand of Eq. (A2) comes through V_n. Following McConnell and Moy [6], Green's theorem [33] is used to transform the double surface integral into a double line integral over the contours C_1 and C_2 surrounding S_1 and S_2, respectively,

$$\int_{S_1}\int_{S_2} d^2r_1 d^2r_2 \left(\frac{\partial^2 G}{\partial x_1 \partial x_2}+\frac{\partial^2 F}{\partial y_1 \partial y_2}\right) = \oint_{C_1}\oint_{C_2}(F dx_1 dx_2 + G dy_1 dy_2).$$

If $F\equiv G$ is only a function of R, we have

$$\int_{S_1}\int_{S_2} d^2r_1 d^2r_2 \nabla_R^2 F = -\oint_{C_1}\oint_{C_2} F \vec{dl}_1\cdot\vec{dl}_2. \quad \text{(A3)}$$

Following Flament and Gallet [23] we introduce the function $P_n(R)$ such that

$$\nabla^2 P_n(R)=\begin{cases} \frac{1}{2}V_n(R) & \text{if } R\geqslant a; \\ 0 & \text{if } R<a. \end{cases} \quad \text{(A4)}$$

For $n\neq 2$, P_n is given by

$$P_n(R)=\begin{cases} A_n\left(\frac{a}{R}\right)^{n-2} & R\geqslant a; \\ A_n\left[1-(n-2)\ln\left(\frac{R}{a}\right)\right] & R<a; \end{cases} \qquad A_n=\frac{K_n}{2(n-2)^2 a^{n-2}}. \quad \text{(A5)}$$

This function and its derivative are continuous at $R=a$. P_n satisfies the required conditions everywhere except at $R=0$, where $\nabla^2 P_n=-2\pi(n-2)A_n\delta^{(2)}(R)$. In the particular case $n=2$, we have $P_2(R)=(K_2/4)[\ln(R/a)]^2$ for $R>a$ and $P_2(R)=0$ for $R<a$. Using the definition of $P_n(R)$ and the Green's theorem [Eq. (A3)], Eq. (A2) can be rewritten as

$$E_n=E_s+E_c=2\pi(n-2)A_n\sigma_1\sigma_2\int_{S_1}\int_{S_2} d^2r_1 d^2r_2\,\delta^{(2)}(R)-\sigma_1\sigma_2\oint_{C_1}\oint_{C_2} P_n(R)\vec{dl}_1\cdot\vec{dl}_2. \quad \text{(A6)}$$

E_n appears as the sum of a surface term E_s and a boundary term E_c. This is readily shown in the following example. Consider a domain with particle density σ_1 and area S_1 embedded in a 2D bulk with particle density σ_2 and area S_2. The energy of this bubblelike system can be written as

$$E_{bubble}=\tfrac{1}{2}\sigma_1^2\int_{S_1}\int_{S} d^2r_1 d^2r_2 V_n+\tfrac{1}{2}\sigma_2^2\int_{S}\int_{S_2} d^2r_1 d^2r_2 V_n-\tfrac{1}{2}(\sigma_1-\sigma_2)^2\int_{S_1}\int_{S_2} d^2r_1 d^2r_2 V_n, \quad \text{(A7)}$$

where $S=S_1+S_2$. Taking the thermodynamic limit ($S_2\to\infty$) for the case $n>2$ and using Eq. (A6) this energy can be decoupled into

$$\begin{aligned} E_{bubble} &= 2\pi(n-2)A_n\sigma_1^2 S_1+2\pi(n-2)A_n\sigma_2^2 S_2-(\sigma_1-\sigma_2)^2\oint_{C_1}\oint_{C_1} P_n(R)\vec{dl}_1\cdot\vec{dl}_2+E_B \\ &= \epsilon_1 S_1+\epsilon_2 S_2-(\sigma_1-\sigma_2)^2\oint_{C_1}\oint_{C_1} P_n(R)\vec{dl}_1\cdot\vec{dl}_2+E_B, \end{aligned} \quad \text{(A8)}$$

where $E_B=-\sigma_2^2\oint_B\oint_B P_n(R)\vec{dl}_1\cdot\vec{dl}_2$ and B is the boundary of the system. ϵ_i is the energy per unit area for a domain of infinite size with particle density σ_i and is given by

$$\epsilon_i=2\pi(n-2)A_n\sigma_i^2\equiv\tfrac{1}{2}\sigma_i^2\int_{r>a} d^2r V_n(r). \quad \text{(A9)}$$

The integral definition of ϵ_i is convergent only for $n>2$. This is consistent with the statement [23] that for a straight boundary, E_c/E_s diverges in the thermodynamic limit for the case $n\leqslant 2$. When the boundary of the system is fixed, E_B is a constant and the relevant energy of this system is

$$\begin{aligned} \Delta E_{bubble} &= E_{bubble}-E_B \\ &= \epsilon_1 S_1+\epsilon_2 S_2-(\sigma_1-\sigma_2)^2\oint_{C_1}\oint_{C_1} P_n(R)\vec{dl}_1\cdot\vec{dl}_2. \end{aligned} \quad \text{(A10)}$$

This analysis for a system of two domains is extended in Sec. II to a system of infinite number of domains in the case

of a supercrystal.

The use of Green's theorem therefore allows a convenient physical picture of interacting boundaries. This simplification will be used in the treatment of the fluctuations of the domain boundaries, where the area of the domains is conserved and the only relevant energy is that of the boundaries.

2. Dipolar case and application to the stripe phase

In the case of dipolar interactions ($n=3$) Eq. (A10) is in agreement with the formalism of McConnell *et al.* [21,34], and differs from it only in the way the microscopic cutoff is introduced. In the latter, the microscopic cutoff is explicitly included in the potential which is written

$$V_{dip}\equiv V_3=\frac{K_d}{\rho^3}, \tag{A11}$$

where $\rho=(R^2+\Delta^2)^{1/2}$ and Δ is the microscopic cutoff. Using this definition implies that $\nabla^2 P=\frac{1}{2}V$ everywhere; thus, P is not restricted as in Eq. (A5). This form simplifies the calculation of the line integrals and we shall use it in the rest of this work [22].

In the treatment of the stripe phase we take (for simplicity) K_d out of the definition of P. We introduce $V(R)=\rho^{-3}$, as defined in Eq. (2.1), and the function $P(R)$ that satisfies $\nabla^2 P(R)=\frac{1}{2}V(R)$. Using Eq. (2.2) the electrostatic part of the energy per cell is written

$$E_{cell}=\epsilon_1 S_1+\epsilon_2 S_2 - \tfrac{1}{2}\mu^2\sum_{j=-\infty}^{\infty}\int_{(0,1)}\int_{(j,2)} d^2r_{(0,1)}d^2r_{(j,2)}V(|\vec{r}_{(0,1)}-\vec{r}_{(j,2)}|). \tag{A12}$$

Using Green's theorem, Eq. (A3), for each of the integrals in Eq. (A12) we obtain a physical picture of interacting boundaries of polarities, which are indicated by the arrows in Fig. 1. The dipolar energy per cell is now written

$$\begin{aligned}E_{cell}&=\epsilon_1 S_1+\epsilon_2 S_2+\mu^2\sum_{j=-\infty}^{\infty}\oint_{(0,1)}\oint_{(j,2)}P(|\vec{r}_{(0,1)}-\vec{r}_{(j,2)}|)\vec{dl}_{(0,1)}\cdot\vec{dl}_{(j,2)}\\ &=\epsilon_1 S_1+\epsilon_2 S_2+\mu^2\sum_{j=-\infty}^{\infty}\int_{-L/2}^{L/2}\int_{-L/2}^{L/2}dx_1dx_2\{P(\sqrt{(j+\phi)^2D^2+(x_1-x_2)^2})+P(\sqrt{(j-\phi)^2D^2+(x_1-x_2)^2})\\ &\quad -2P(\sqrt{(jD)^2+(x_1-x_2)^2})\},\end{aligned} \tag{A13}$$

where in the last step we used the fact that in the thermodynamic limit (i.e., $L\to\infty$) the only significant contribution to the line integrals comes from the boundaries parallel to the stripes. Since these are line integrals, each boundary has a ''polarity'' (up or down) as indicated by the arrows in Fig. 1. The interaction energy between two antiparallel boundaries separated by a distance $w\ll L$ is

$$\begin{aligned}E(w)&=-\mu^2\int_{-L/2}^{L/2}\int_{-L/2}^{L/2}dx_1dx_2P(\sqrt{(x_1-x_2)^2+w^2})\\ &=\begin{cases}-\mu^2 L\,\ln\left(\dfrac{2L}{we}\right) & \text{if } w\gg\Delta;\\ -\mu^2 L\,\ln\left(\dfrac{2L}{\Delta}\right) & \text{if } w=0.\end{cases}\end{aligned} \tag{A14}$$

The boundary-boundary interaction kernel is written $P=\frac{1}{2}\rho^{-1}$ for $\rho\gg\Delta$, which is always correct for $w\gg\Delta$. The case $w=0$, which may be referred to as the self-energy of the boundary, corresponds to the last term of Eq. (A13) with $j=0$. In this case a multipole correction term, which is $-\mu^2$ per unit length, must be taken into account as shown by McConnell and de Koker [21,35].

Using Eq. (A14) for each of the terms in the sum in Eq. (A13), and using the identity

$$\sin(\pi\phi)=(\pi\phi)\prod_{n=1}^{\infty}\left[1-\left(\frac{\phi}{n}\right)^2\right], \tag{A15}$$

we finally obtain Eq. (2.3),

$$E_{cell}=LD[\phi\epsilon_1+(1-\phi)\epsilon_2]-2L\mu^2\left[\ln\frac{D}{\Delta}+1+\ln\frac{\sin(\pi\phi)}{\pi}\right]. \tag{A16}$$

APPENDIX B: FLUCTUATIONS OF TWO BOUNDARIES

The use of Green's theorem gives a physical picture of interacting boundaries through some pair potential. Thus, in order to analyze the fluctuating stripe phase we consider the case of two fluctuating boundaries. This analysis is extended to the stripe phase in Appendix C. As in Appendix A we start with the more general case and consider a power-law interaction V_n as defined in Eq. (A1). In Sec. II it was shown that the interactions are reduced to line integrals over straight and parallel boundaries. We now consider two such boundaries of length L, separated by a distance w (the case $w=0$ was treated by Flament and Gallet [23]) and let them fluctuate about their equilibrium positions with small perturbations $y_1(x_1)$ and $y_2(x_2)$ with $\langle y_i\rangle_{x_i}=0$. Due to the extra line length $\vec{dl}_i$ has now a component in the $\hat{y}$ direction and be-

comes $\vec{dl}_i = \pm dx_i(\hat{\vec{x}} + dy_i/dx_i\,\hat{\vec{y}})$, where the plus sign corresponds to a down arrow boundary and the minus to an up one (see Fig. 1). The interaction energy of two antiparallel boundaries separated by an average distance w as in Eq. (A14) becomes

$$E_n(w) = -\mu^2 \int_{-L/2}^{L/2}\int_{-L/2}^{L/2} dx_1 dx_2 \times P_n(\sqrt{(x_2-x_1)^2+(w+y_2-y_1)^2})\left(1+\frac{dy_1}{dx_1}\frac{dy_2}{dx_2}\right). \tag{B1}$$

[In order to be consistent with the notation of Appendix A and Sec. II we have $\mu^2=(\sigma_1-\sigma_2)^2$ for $n\neq 3$ and $\mu^2=(\sigma_1-\sigma_2)^2K_d$ for $n=3$.] After expanding P_n up to second order in y and assuming $dy_i/dx_i \ll 1$ one finds $E_n(w)=E_n^0(w)+\Delta E_n(w)$, where $E_n^0(w)$ is the interaction energy of the straight boundaries, and $\Delta E_n(w)$ is the fluctuation energy, given by

$$\Delta E_n(w) = -\mu^2 \int_A dx_1 dx_2 \left[\frac{dy_1}{dx_1}\frac{dy_2}{dx_2}P_n(r) + \frac{1}{r}\frac{1}{2}(y_1-y_2)^2\left(1-\frac{w^2}{r^2}\right)\frac{\partial P_n(r)}{\partial r} + \tfrac{1}{2}(y_1-y_2)^2\frac{w^2}{r^2}\frac{\partial^2 P_n(r)}{\partial r^2} + (y_2-y_1)\frac{w}{r}\frac{\partial P_n(r)}{\partial r}\right]. \tag{B2}$$

Here, $r=\sqrt{(x_1-x_2)^2+w^2}$ and the double line integral is now considered as a surface integral over a square of area $A=L^2$. The integral in the last term of $\Delta E_n(w)$ vanishes for $n>2$ in the thermodynamic limit, since the average value of the fluctuations is zero. Applying Green's theorem again we obtain

$$\Delta E_n(w) = -\tfrac{1}{2}\mu^2\left\{\int_A dx_1 dx_2 (y_1-y_2)^2\nabla^2 P_n - \oint_B dx_1 \frac{\partial}{\partial x_1}[(y_1-y_2)^2 P_n] + \oint_B dx_1\left[\frac{\partial}{\partial x_1}(y_1-y_2)^2\right]P_n - \oint_B dx_2\left[\frac{\partial}{\partial x_2}(y_1-y_2)^2\right]P_n\right\}, \tag{B3}$$

where B represents the contour of the square A. Using periodic boundary conditions $y(-L/2)=y(L/2)$ the second integral is found to be independent of the system size, L, in the thermodynamic limit and hence negligible with respect to the first one. The second integral vanishes identically for $w=0$ as argued by Flament and Gallet [23]. The $w=0$ equivalents for the last two integrals do not appear in their results. We find that these two integrals are also negligible in the thermodynamic limit with respect to the first one for $n>2$. Thus, for $n>2$ we are left in the thermodynamic limit with

$$\Delta E_n(w) = -\tfrac{1}{2}\mu^2\int_A dx_1 dx_2 (y_1-y_2)^2\nabla^2 P_n(r) = -\tfrac{1}{4}\mu^2\int_A dx_1 dx_2 (y_1-y_2)^2 V_n(r). \tag{B4}$$

Expanding y_i in the Fourier series, $y_i(x_i)=(1/\sqrt{L})\sum_q y_{i_q} e^{iqx_i}$, we obtain in the thermodynamic limit

$$\Delta E_n(w) = \tfrac{1}{4}\mu^2\left\{\sum_q [\tilde{V}_n(q,w)+\tilde{V}_n(-q,w)] y_{1_q} y_{2_q}^* - \sum_q (|y_{1_q}|^2+|y_{2_q}|^2)\tilde{V}_n(0,w)\right\}, \tag{B5}$$

where $\tilde{V}_n(q,w)\equiv\int_{-\infty}^{+\infty} du V_n(\sqrt{u^2+w^2})e^{iqu}$.

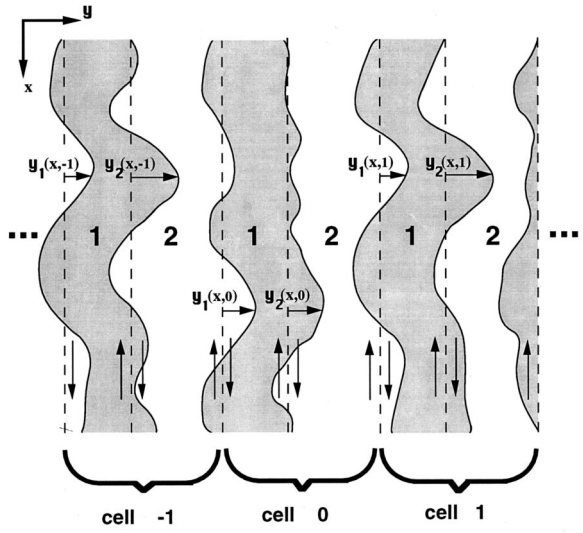

FIG. 6. The fluctuating stripe phase. The equilibrium positions of the stripe boundaries are shown in dashed lines. Each boundary fluctuates with an amplitude $y_m(x,i)$, where i is the cell index and $m=1,2$ is the boundary index within the cell. Using Green's theorem, the dipolar fluctuation energy is represented by double line integrals that correspond to boundary-boundary interactions. The interactions are between boundaries of stripes labeled 1 and stripes labeled 2. Each boundary has a ''polarity,'' indicated by an arrow, that corresponds to the direction of integration along this boundary.

APPENDIX C: NORMAL MODE ANALYSIS OF THE FLUCTUATING STRIPE PHASE

In this Appendix we consider the fluctuations of the boundaries of the stripes about their equilibrium positions, assigning an independent small perturbation with a zero average to each of the boundaries, as shown in Fig. 6. We derive an expression for the fluctuation free energy, that leads to two branches (acoustic and optical) in the energy spectrum.

In Sec. II we treated the stripe phase in equilibrium and considered the energy per cell in Eq. (2.2), which was possible due to the symmetry of this phase. However, when we

treat the fluctuations of this phase we must consider the total fluctuation energy. Using the (j,n) notation of Eq. (2.2) we find

$$E_{dip}=\frac{1}{2}\sum_{m,n=1}^{2}\sum_{i,j=-\infty}^{+\infty}\sigma_m\sigma_n K_d\int_{(i,m)}\int_{(j,n)}d^2r_{(i,m)}d^2r_{(j,n)}\times V(|\vec{r}_{(i,m)}-\vec{r}_{(j,n)}|)$$
$$=E_b+\mu^2\sum_{i,j=-\infty}^{+\infty}\oint_{(i,1)}\oint_{(j,2)}\times P(|\vec{r}_{(i,1)}-\vec{r}_{(j,2)}|)\vec{dl}_{(i,1)}\cdot\vec{dl}_{(j,2)}, \quad \text{(C1)}$$

where $E_b=\epsilon_1A_1+\epsilon_2A_2$ and $\mu^2=(\sigma_1-\sigma_2)^2K_d$. A_1 and A_2 are the total areas of the stripes with dipolar densities σ_1 and σ_2, and energy densities ϵ_1 and ϵ_2, respectively. These areas are fixed since the perturbations have a zero average and thus E_b is the equilibrium bulk energy. Each of the contour integrals in Eq. (C1) can be divided into two line integrals [of the same form that was considered in Eq. (B1) for two fluctuating boundaries], since in the thermodynamic limit the contribution from the ends of the stripes is negligible. Subtracting the total equilibrium energy of the stripe phase and using Eq. (B4), the relevant electrostatic energy for the analysis of the fluctuations is written

$$\Delta E_{dip}=E_{dip}-E_{equilibrium}=\sum_{i,j=-\infty}^{+\infty}\sum_{n,m=1}^{2}(-1)^{m+n}\times\Delta E^{i,n}_{j,m}([j-i+(m-n)\phi]D)$$
$$\equiv-\tfrac{1}{4}\mu^2\sum_{i,j=-\infty}^{+\infty}\sum_{n,m=1}^{2}(-1)^{m+n}\int_{-L/2}^{L/2}\int_{-L/2}^{L/2}dx_1dx_2\times[y_m(x_1,j)-y_n(x_2,i)]^2\times V(\sqrt{(x_1-x_2)^2+[j-i+(m-n)\phi]^2D^2}), \quad \text{(C2)}$$

where $V(R)$ was defined in Eq. (2.1) and using the definition of the equilibrium dipolar energy per cell in Eq. (2.3) we have $E_{equilibrium}=$ (number of cells)$\times E_{cell}$. The boundary fluctuation amplitudes are denoted $y_m(x,i)$, where i is the cell index and $m=1,2$ is the boundary index within the cell, as shown in Fig. 6. The indices $(i,n),(j,m)$ were attached to ΔE in order to label the boundaries 1,2 that appear in Eq. (B4). We diagonalize this quadratic form of the energy by transforming both the x coordinate and the discrete coordinates j,i into Fourier space. For x we write $y_m(x,j)=(1/\sqrt{L})\,\Sigma_q y_m(q,j)e^{iqx}$, where $q\in(-\pi/\Delta,\pi/\Delta)$. For j we introduce a discrete Fourier transform in the $\hat{\tilde{y}}$ direction (perpendicular to the stripes)

$$\tilde{Y}_m(q,Q)=\frac{1}{\sqrt{N}}\sum_j y_m(q,j)e^{ijDQ};$$

$$y_m(q,j)=\frac{1}{\sqrt{N}}\sum_Q \tilde{Y}_m(q,Q)e^{-ijDQ}, \quad \text{(C3)}$$

where N is the number of cells and $Q\in(-\pi/D,\pi/D)$ lies in the first Brillouin zone of the reciprocal lattice of the supercrystal. We include in the boundary energy the microscopic line tension γ [see Eq. (2.4)] and the resulting fluctuation Hamiltonian is written

$$\Delta H=\frac{1}{2}\sum_q\sum_Q\tilde{Y}(q,Q)\tilde{\mathcal{G}}(q,Q)\tilde{Y}^{\dagger}(q,Q), \quad \text{(C4)}$$

where $\tilde{Y}(q,Q)=(\tilde{Y}_1(q,Q),\tilde{Y}_2(q,Q))$ is a row vector and $\tilde{\mathcal{G}}$ is a 2×2 matrix, whose detailed derivation is given in Appendix D,

$$\tilde{\mathcal{G}}(q,Q)=\tilde{\mathcal{B}}(q,Q)+\mathbb{1}(\gamma q^2-\mathcal{B}_0), \quad \text{(C5a)}$$

where

$$\tilde{\mathcal{B}}(q,Q)=\frac{2\pi\mu^2}{\Delta D}\sum_{k=-\infty}^{+\infty}e^{-(\Delta/D)\sqrt{(2\pi k+QD)^2+(qD)^2}}\times\begin{pmatrix}1 & -e^{-i\phi(2\pi k+QD)}\\ -e^{i\phi(2\pi k+QD)} & 1\end{pmatrix} \quad \text{(C5b)}$$

and $\mathcal{B}_0$ is a positive function of ϕ, which is written

$$\mathcal{B}_0=\frac{1}{2}\sum_{m,n=1}^{2}\tilde{\mathcal{B}}_{mn}(0,0)=\frac{4\pi\mu^2}{\Delta D}\sum_{k=-\infty}^{+\infty}\sin^2(\pi k\phi)e^{-(\Delta/D)\,2\pi k}. \quad \text{(C5c)}$$

Using Eqs. (C5) the fluctuation Hamiltonian of Eq. (C4) can be schematically rewritten as

$$\Delta H=\frac{1}{2}\sum_q\sum_Q(\tilde{Y}_1(q,Q)\quad\tilde{Y}_2(q,Q))\times\begin{pmatrix}\tilde{\mathcal{G}}_1(q,Q) & \tilde{\mathcal{G}}_2(q,Q)\\ \tilde{\mathcal{G}}_2^*(q,Q) & \tilde{\mathcal{G}}_1(q,Q)\end{pmatrix}\begin{pmatrix}\tilde{Y}_1^*(q,Q)\\ \tilde{Y}_2^*(q,Q)\end{pmatrix}, \quad \text{(C6)}$$

where

$$\tilde{\mathcal{G}}_1(q,Q)=\frac{2\pi\mu^2}{\Delta D}\sum_{k=-\infty}^{+\infty}e^{-(\Delta/D)\sqrt{(2\pi k+QD)^2+(qD)^2}}+\gamma q^2-\mathcal{B}_0, \quad \text{(C7a)}$$

and

$$\tilde{\mathcal{G}}_2(q,Q)=-\frac{2\pi\mu^2}{\Delta D}\sum_{k=-\infty}^{+\infty}e^{-(\Delta/D)\sqrt{(2\pi k+QD)^2+(qD)^2}}\times e^{-i\phi(2\pi k+QD)}. \quad \text{(C7b)}$$

Thus, the problem is reduced to that of pairs of coupled oscillators. We decouple the oscillators through diagonalization of Eq. (C6), which yields

$$\Delta H=\frac{1}{2}\sum_q\sum_Q[\tilde{\mathcal{G}}_+(q,Q)|\tilde{\mathcal{Y}}_+(q,Q)|^2+\tilde{\mathcal{G}}_-(q,Q)|\tilde{\mathcal{Y}}_-(q,Q)|^2], \quad \text{(C8)}$$

where

$$\tilde{\mathcal{G}}_{\pm}(q,Q)=\tilde{\mathcal{G}}_1(q,Q)\pm|\tilde{\mathcal{G}}_2(q,Q)|, \tag{C9a}$$

$$\tilde{\mathcal{Y}}_{\pm}(q,Q)=\frac{1}{\sqrt{2}}[\tilde{Y}_2(q,Q)\pm e^{i\theta}\tilde{Y}_1(q,Q)] \tag{C9b}$$

and

$$e^{i\theta(q,Q,\phi)}=\frac{\tilde{\mathcal{G}}_2(q,Q)}{|\tilde{\mathcal{G}}_2(q,Q)|};\quad \lim_{QD\to 0}\theta(q,Q,\phi)=\pi. \tag{C9c}$$

$\mathcal{G}_+$ and $\mathcal{G}_-$ correspond to the optical and acoustic branches of the energy spectrum, respectively ($\mathcal{G}_-$ vanishes in the limit $qD,QD\to 0$). It is important to note that Eq. (C9c) implies that in the limit $QD\to 0$ the acoustic and optical branches coincide with symmetric and antisymmetric modes of the stripes, respectively.

This general form of the second-order fluctuation Hamiltonian will be further analyzed in order to calculate physical quantities. However, an important property of the system can already be extracted from this expression: The $\tilde{Y}(q,Q)$ are not eigenvectors of the system, nor are (with the exception of the $Q=0$ case) the symmetric and antisymmetric modes of the stripes ($\tilde{Y}_1(q,Q)+\tilde{Y}_2(q,Q),\tilde{Y}_2(q,Q)-\tilde{Y}_1(q,Q)$). Thus, any separate analysis of the only symmetric or antisymmetric modes neglects their coupling and is only an approximation, which becomes a good one only at long wavelengths ($Q\to 0$). Infinite wavelength (in the $\hat{\vec{y}}$ direction, $Q=0$) symmetric or antisymmetric modes, for which these modes do decouple, were considered by several authors [10,16–18] in the context of stability of the supercrystal. However, these $Q=0$ modes cost a macroscopic amount of energy, which makes them improbable, and hence one must consider finite Q modes in calculating physical quantities.

APPENDIX D: THE KERNEL OF THE GENERAL FLUCTUATION HAMILTONIAN

In this Appendix we derive $\tilde{\mathcal{G}}(q,Q)$, the kernel of the second-order fluctuation Hamiltonian of the stripe supercrystal, as it appears in Eq. (C4) .

We first expand the perturbations of the boundaries in the Fourier series, $y_m(x,j)=(1/\sqrt{L})\,\Sigma_q y_m(q,j)e^{iqx}$, and use Eq. (B5) to rewrite the electrostatic fluctuation energy of Eq. (C2) as

$$\Delta E_{dip}=\frac{1}{2}\sum_q\sum_{i,j}Y(q,i)\mathcal{C}(q,j-i)Y^{\dagger}(q,j), \tag{D1}$$

where $Y(q,i)=(y_1(q,i),y_2(q,i))$ is a row vector and $\mathcal{C}$ is a 2×2 matrix. Note that due to the discrete translational symmetry of the supercrystal, $\mathcal{C}$ is a function of $j-i$ and we denote $l\equiv j-i$. Using the definition of $V(R)$ in Eq. (2.1) we introduce the one-dimensional ($\hat{\vec{x}}$ direction) Fourier transform of $V(\sqrt{x^2+w^2})$, such that $\tilde{V}(q,w)\equiv\int_{-\infty}^{+\infty}duV(\sqrt{u^2+w^2})e^{iqu}$. Using that $\Sigma_{p=-\infty}^{\infty}\tilde{V}(0,(p-\phi)D)=\Sigma_{p=-\infty}^{\infty}\tilde{V}(0,(p+\phi)D)$ we obtain

$$\begin{aligned}\mathcal{C}_{1,1}(q,0)&=\mathcal{C}_{2,2}(q,0)\\&=\frac{1}{2}\mu^2 b\Bigg\{\sum_{p=-\infty}^{\infty}[[\tilde{V}(0,(p-\phi)D)\\&\quad+\tilde{V}(0,(p+\phi)D)]-2\tilde{V}(0,pD)]\\&\quad+[\tilde{V}(q,0)+\tilde{V}(-q,0)]\Bigg\};\end{aligned}$$

$$\mathcal{C}_{1,1}(q,l\neq 0)=\mathcal{C}_{2,2}(q,l\neq 0)=\tfrac{1}{2}\mu^2[\tilde{V}(q,lD)+\tilde{V}(-q,lD)];$$

$$\mathcal{C}_{1,2}(q,l)=-\tfrac{1}{2}\mu^2[\tilde{V}(q,(l+\phi)D)+\tilde{V}(-q,(l+\phi)D)];$$

$$\mathcal{C}_{2,1}(q,l)=-\tfrac{1}{2}\mu^2[\tilde{V}(q,(l-\phi)D)+\tilde{V}(-q,(l-\phi)D)]. \tag{D2}$$

We define $\mathcal{B}(q,l)$ such that

$$\mathcal{B}_{1,1}=\mathcal{B}_{2,2}=\tfrac{1}{2}\mu^2[\tilde{V}(q,lD)+\tilde{V}(-q,lD)];$$

$$\mathcal{B}_{1,2}=\mathcal{C}_{1,2};$$

$$\mathcal{B}_{2,1}=\mathcal{C}_{2,1}, \tag{D3}$$

with its discrete Fourier transform

$$\tilde{\mathcal{B}}(q,Q)=\sum_{m=-\infty}^{\infty}\mathcal{B}(q,m)e^{imDQ}. \tag{D4}$$

Using the above definitions Eq. (D2) is rewritten

$$\mathcal{C}(q,l)=\mathcal{B}(q,l)-\mathbb{1}\delta_{l,0}\mathcal{B}_0, \tag{D5}$$

where $\delta_{l,r}$ is the delta of Kronecker, $\mathbb{1}$ is a 2×2 unit matrix, and $\mathcal{B}_0$ is a positive function of ϕ, which was defined in Eq. (C5c). We add to the dipolar energy the microscopic short-range attractions through the line tension γ. Using the notation of Eq. (D1) the fluctuation energy due to the line tension is written

$$\Delta E_{\gamma}=\frac{1}{2}\gamma\sum_q\sum_{i,j}\delta_{l,0}q^2Y(q,i)Y^{\dagger}(q,j), \tag{D6}$$

where again $l\equiv j-i$. Using Eqs. (D1) and (D6) we obtain the total fluctuation Hamiltonian,

$$\Delta H=\Delta E_{dip}+\Delta E_{\gamma}=\frac{1}{2}\sum_q\sum_{i,j}Y(q,i)\mathcal{G}(q,l)Y^{\dagger}(q,j), \tag{D7}$$

where using Eqs. (D5) and (D6) we find

$$\mathcal{G}(q,l)=\mathcal{B}(q,l)+\mathbb{1}\delta_{l,0}(\gamma q^2-\mathcal{B}_0). \tag{D8}$$

Using Eq. (C3) we represent the boundary perturbations $Y(q,i)$ in Eq. (D7) as a Fourier series in Q space. We transform the summation indices from (i,j) to (l,j). Thus we obtain the full Fourier representation of the fluctuation Hamiltonian, Eq. (C4), with the kernel

$$\tilde{\mathcal{G}}(q,Q)=\sum_{p=-\infty}^{\infty}\tilde{\mathcal{G}}(q,p)e^{ipDQ}=\tilde{\mathcal{B}}(q,Q)+\mathbb{1}(\gamma q^2-\mathcal{B}_0). \tag{D9}$$

We use the method that was developed in Appendix E in order to extend $\tilde{\mathcal{B}}(q,Q)$ from $\tilde{\mathcal{B}}(q,0)$. Using Eq. (D4) and a Gaussian representation for the potential

$$V(R)=[R^2+\Delta^2]^{-3/2}=-\frac{4}{\sqrt{\pi}}\frac{\partial}{\partial(\Delta^2)}\int_0^\infty dt e^{-(R^2+\Delta^2)t^2}, \tag{D10}$$

in Eq. (D3) we obtain

$$\tilde{\mathcal{B}}(q,0)=\sum_{m=-\infty}^{\infty}\mathcal{B}(q,m)$$
$$=-\frac{2\mu^2}{\sqrt{\pi}}\frac{\partial}{\partial(\Delta^2)}\int_{-\infty}^{\infty}du(e^{iqu}+e^{-iqu})\int_0^\infty dt\mathcal{A}(t,u), \tag{D11}$$

where $\mathcal{A}(t,u)$ is a 2×2 matrix

$$\mathcal{A}_{r,l}(t,u)=(-1)^{r+l}\sum_{m=-\infty}^{\infty}\exp\left\{-\left[u^2+(2\pi m+2\pi a_{r,l})^2\left(\frac{D}{2\pi}\right)^2+\Delta^2\right]t^2\right\}, \tag{D12}$$

and $a_{r,l}=(l-r)\phi$. Using the Poisson summation formula, Eq. (E5), for Eq. (D12) we obtain

$$\mathcal{A}_{r,l}(t,u)=\frac{\sqrt{\pi}}{D}e^{-(u^2+\Delta^2)t^2}(-1)^{r+l}\times\sum_{k=-\infty}^{\infty}\exp\left[-\left(\frac{\pi k}{tD}\right)^2-i2\pi k a_{r,l}\right]. \tag{D13}$$

Introducing Eq. (D13) in Eq. (D11) we obtain

$$\tilde{\mathcal{B}}_{r,l}(q,0)=-\frac{2\mu^2}{D}(-1)^{r+l}\sum_{k=-\infty}^{\infty}e^{-i2\pi k a_{r,l}}\times\int_0^\infty dt\ t^{-1}\frac{\partial}{\partial(\Delta^2)}[e^{-\Delta^2t^2}]e^{-(\pi k/tD)^2}\times\int_{-\infty}^{\infty}du(e^{iqu}+e^{-iqu})e^{-t^2u^2}$$
$$=\frac{4\sqrt{\pi}\mu^2}{D}(-1)^{r+l}\sum_{k=-\infty}^{\infty}e^{-i2\pi k a_{r,l}}\int_0^\infty dt\times\exp\left\{-\Delta^2t^2-\frac{1}{4}\left[\left(\frac{2\pi k}{D}\right)^2+q^2\right]t^{-2}\right\}, \tag{D14}$$

which gives after some calculus

$$\tilde{\mathcal{B}}_{r,l}(q,0)=\frac{2\pi\mu^2}{\Delta D}(-1)^{r+l}\times\sum_{k=-\infty}^{\infty}e^{-(\Delta/D)\sqrt{(2\pi k)^2+(qD)^2}}e^{-i2\pi k a_{r,l}}. \tag{D15}$$

Comparing the definition of $\tilde{\mathcal{B}}$ in Eq. (D4) with Eq. (E2), we identify W in our case as $QD/2\pi$. [Equations (E2) and (E5) require the argument to be $2\pi m$, while the argument of $\mathcal{B}$ in Eqs. (D4) and (D11) is m. We achieve the proper form of the argument by transforming $m\to 2\pi m$ together with $D\to D/2\pi$, as is done in Eq. (D12).] Using Eq. (E4) we substitute k with $k+QD/2\pi$ in Eq. (D15) and extend $\tilde{\mathcal{B}}(q,Q)$ from $\tilde{\mathcal{B}}(q,0)$,

$$\tilde{\mathcal{B}}_{r,l}(q,Q)=\frac{2\pi\mu^2}{\Delta D}(-1)^{r+l}\times\sum_{k=-\infty}^{\infty}e^{-(\Delta/D)\sqrt{(2\pi k+QD)^2+(qD)^2}}\times e^{-i(2\pi k+QD)a_{r,l}}. \tag{D16}$$

Substituting $a_{r,l}=(l-r)\phi$ we finally obtain Eq. (C5b).

APPENDIX E: THE EXTENDED POISSON SUMMATION FORMULA

In this Appendix we find the relation between the continuous Fourier transformation of a function and the discrete Fourier transformation of the same function evaluated at discrete points. Consider the continuous function $h(x)$ with the Fourier transform

$$\hat{H}(\eta)=\frac{1}{2\pi}\int_{-\infty}^{\infty}dx e^{i\eta x}h(x);$$
$$h(x)=\int_{-\infty}^{\infty}d\eta e^{-i\eta x}\hat{H}(\eta), \tag{E1}$$

as well as the same function evaluated at discrete points $x=2\pi m$ with the discrete Fourier transformation

$$\tilde{H}(W)=\sum_{m=-\infty}^{\infty}e^{i2\pi mW}h(2\pi m). \tag{E2}$$

Using the Poisson summation formula, Eq. (E5), with $h(2\pi m)=\delta(\eta-m)$ we find

$$\sum_{k=-\infty}^{\infty}\delta(\eta-k)=\sum_{m=-\infty}^{\infty}e^{-i2\pi m\eta}. \tag{E3}$$

Using this identity together with Eq. (E1), Eq. (E2) is rewritten

$$\widetilde{H}(W)=\sum_{m=-\infty}^{\infty} e^{i2\pi mW}\int_{-\infty}^{\infty} d\eta e^{-i2\pi m\eta}\hat{H}(\eta)$$
$$=\int_{-\infty}^{\infty} d\eta \hat{H}(\eta)\sum_{k=-\infty}^{\infty}\delta(\eta-W-k)$$
$$=\sum_{k=-\infty}^{\infty}\hat{H}(k+W). \tag{E4}$$

This equality reduces in the case of $W=0$ to the Poisson summation formula (see, for example, Ref. [36]),

$$\widetilde{H}(0)=\sum_{m=-\infty}^{+\infty} h(2\pi m)=\sum_{k=-\infty}^{\infty}\hat{H}(k). \tag{E5}$$

Hence, it is possible to extend $\widetilde{H}(W)$ from $\widetilde{H}(0)$ by merely substituting $k+W$ for k in the argument of $\hat{H}$ in the Poisson summation formula.

APPENDIX F: FLUCTUATION HAMILTONIAN FOR SYMMETRIC MODES

In this Appendix we calculate the kernel $\widetilde{G}(q,Q)$ for the fluctuation Hamiltonian of the symmetric modes, ΔH_s, and find its long wavelength approximation (i.e., its value in the limit $qD,QD\ll 1$).

Our model contains only symmetric modes and therefore we have only one degree of freedom per cell. Thus, Eq. (C4) for the full fluctuation Hamiltonian reduces to Eq. (3.1),

$$\Delta H_s=\frac{1}{2}\sum_{q,Q}|\widetilde{y}(q,Q)|^2\widetilde{G}(q,Q), \tag{F1}$$

where

$$\widetilde{G}(q,Q)=\sum_{m,n=1}^{2}\widetilde{\mathcal{G}}_{m,n}(q,Q). \tag{F2}$$

Using the definition of $\widetilde{\mathcal{G}}(q,Q)$ in Eqs. (C5) we obtain

$$\widetilde{G}(q,Q)=\widetilde{F}(q,Q)-\widetilde{F}(0,0)+2\gamma q^2, \tag{F3}$$

where

$$\widetilde{F}(q,Q)=\sum_{m,n=1}^{2}\widetilde{\mathcal{B}}_{m,n}(q,Q)=\frac{8\pi\mu^2}{\Delta D}\sum_{k=-\infty}^{\infty}\sin^2\left[(2\pi k+QD)\frac{\phi}{2}\right]e^{-(\Delta/D)\sqrt{(2\pi k+QD)^2+(qD)^2}}. \tag{F4}$$

Separating the sum in Eq. (F4) we obtain

$$\widetilde{F}(q,Q)=\widetilde{F}_0(q,Q)+\widetilde{Z}(q,Q)+\widetilde{Z}(q,-Q), \tag{F5}$$

where

$$\widetilde{F}_0(q,Q)=\frac{8\pi\mu^2}{\Delta D}\sin^2(\tfrac{1}{2}QD\phi)e^{-(\Delta/D)\sqrt{(QD)^2+(qD)^2}} \tag{F6}$$

is the $k=0$ term and

$$\widetilde{Z}(q,Q)=\frac{8\pi\mu^2}{\Delta D}\sum_{k=1}^{\infty}\sin^2\left[(2\pi k+QD)\frac{\phi}{2}\right]\exp\left[-\frac{\Delta}{D}(2\pi k+QD)\sqrt{1+\left(\frac{qD}{2\pi k+QD}\right)^2}\right]. \tag{F7}$$

In the long wavelength regime $qD,QD\ll 1$, and the exponent in Eq. (F7) can be expanded for $qD\ll 2\pi k+QD$, since $|QD|\leq\pi$ and $k\geq 1$. We thus write

$$\widetilde{Z}(q,Q)=\widetilde{Z}(0,Q)+\widetilde{Z}_2(Q)(qD)^2+\widetilde{Z}_4(qD)^4+\text{higher order terms.} \tag{F8}$$

Denoting $\epsilon=\Delta/D$ which is a small parameter, we find

$$\widetilde{Z}(0,Q)=\frac{8\pi\mu^2}{\Delta D}\sum_{k=1}^{\infty}\sin^2\left[(2\pi k+QD)\frac{\phi}{2}\right]e^{-\epsilon(2\pi k+QD)}, \tag{F9}$$

$$\widetilde{Z}_2(Q)=\frac{1}{2}\frac{\partial^2\widetilde{Z}(q,Q)}{\partial(qD)^2}\bigg|_{q=0}=-\frac{4\pi\mu^2}{D^2}\sum_{k=1}^{\infty}\frac{\sin^2\left[(2\pi k+QD)\frac{\phi}{2}\right]}{2\pi k+QD}e^{-\epsilon(2\pi k+QD)}, \tag{F10}$$

$$\widetilde{Z}_4=\frac{1}{24}\frac{\partial^4\widetilde{Z}(q,Q)}{\partial(qD)^4}\bigg|_{q=Q=0}=\frac{\mu^2}{8\pi^2D^2}\sum_{k=1}^{\infty}\frac{\sin^2(\pi k\phi)}{k^3}e^{-\epsilon 2\pi k}(1+\epsilon 2\pi k). \tag{F11}$$

Using Eq. (F8), Eq. (F5) becomes

$$\widetilde{F}(q,Q)=\widetilde{F}_0(q,Q)+\widetilde{F}(0,Q)+\widetilde{F}_2(Q)(qD)^2+\widetilde{F}_4(qD)^4+\text{higher-order terms}, \tag{F12}$$

where

$$\widetilde{F}(0,Q)=\widetilde{Z}(0,Q)+\widetilde{Z}(0,-Q), \tag{F13}$$

$$\widetilde{F}_2(Q)=\widetilde{Z}_2(Q)+\widetilde{Z}_2(-Q), \tag{F14}$$

$$\widetilde{F}_4=2\widetilde{Z}_4. \tag{F15}$$

For the calculation of $\widetilde{F}(0,Q)$ we represent the sine in Eq. (F9) in terms of exponents and obtain a geometric series which sums to

$$\widetilde{F}(0,Q)=\frac{4\pi\mu^2}{\Delta D}\left\{\frac{2\cosh(\epsilon QD)}{e^{2\pi\epsilon}-1}-\frac{1}{2}\frac{\cos[\phi(2\pi+QD)]e^{-\epsilon QD}+\cos[\phi(2\pi-QD)]e^{\epsilon QD}-2e^{-2\pi\epsilon}\cos(\phi QD)\cosh(\epsilon QD)}{\cosh(2\pi\epsilon)-\cos(2\pi\phi)}\right\}. \tag{F16}$$

Noting that $\widetilde{F}_0(0,0)=0$, we conclude from Eq. (F12) that the only contribution to $\widetilde{F}(0,0)$ comes from the term $\widetilde{F}(0,Q)$. By expanding their difference in ϵ we find using Eq. (F16)

$$\begin{aligned}\widetilde{F}(0,Q)-\widetilde{F}(0,0)&=\frac{4\pi\mu^2}{D^2}\left\{-2\sin^2(\tfrac{1}{2}QD\phi)\epsilon^{-1}\right.\\&\left.+\left[\frac{1}{2\pi}(QD)^2+2\pi\sin^2(\tfrac{1}{2}QD\phi)\sin^{-2}(\pi\phi)-(QD)\cot(\pi\phi)\sin(QD\phi)\right]\epsilon^0+O(\epsilon)\right\}.\end{aligned} \tag{F17}$$

Expanding $\widetilde{F}_0(q,Q)$ in ϵ and using Eq. (F6) we find

$$\widetilde{F}_0(q,Q)=\frac{4\pi\mu^2}{D^2}\{-2\sin^2(\tfrac{1}{2}QD\phi)[\epsilon^{-1}-\sqrt{(QD)^2+(qD)^2}\epsilon^0+O(\epsilon)]\}. \tag{F18}$$

The ϵ^{-1} term of $\widetilde{F}_0(q,Q)$ is thus canceled by that of Eq. (F17) when both are introduced in Eq. (F3). In the long wavelength approximation $QD\ll 1$ and we neglect the ϵ^0 term of Eq. (F18), which is third order in qD,QD with respect to the ϵ^0 term of Eq. (F17), which is of order $(QD)^2$. Thus, using the definition of B_0 in Eq. (3.3b),

$$B_0(\phi)=2[1+\mathrm{sinc}^{-2}(\pi\phi)-2(\pi\phi)\cot(\pi\phi)],$$

we find

$$\widetilde{F}_0(q,Q)+\widetilde{F}(0,Q)-\widetilde{F}(0,0)=\frac{\mu^2}{D^2}B_0(\phi)(QD)^2+\text{higher order terms in }\epsilon,\ qD,\ \text{and}\ QD. \tag{F19}$$

We now consider the fourth-order term. Using Eqs. (F15), (F11), and the definition of K_0 in Eq. (3.3a),

$$K_0(\phi)=\frac{1}{4\pi^2}\sum_{k=1}^{+\infty}\frac{\sin^2(\pi k\phi)}{k^3},$$

we find

$$\widetilde{F}_4=\frac{\mu^2}{D^2}[K_0+O(\epsilon)]. \tag{F20}$$

Finally, we consider $\widetilde{F}_2$. Using Eq. (F14) and expanding Eq. (F10) in QD we find

$$\begin{aligned}\widetilde{F}_2(Q)=&-\frac{4\mu^2}{D^2}\sum_{k=1}^{\infty}\frac{\sin^2(\pi k\phi)}{k}e^{-\epsilon 2\pi k}\\&-(QD)^2\frac{8\pi\mu^2}{D^2}\left\{\sum_{k=1}^{\infty}\left[-\frac{\phi}{2}\frac{\sin(2\pi k\phi)}{(2\pi k)^2}+\frac{\sin^2(\pi k\phi)}{(2\pi k)^3}+\frac{\phi^2}{4}\frac{\cos(2\pi k\phi)}{(2\pi k)^2}\right]+O(\epsilon)\right\}\\&+O((QD)^4).\end{aligned} \tag{F21}$$

Introducing this result back in Eq. (F12) yields a $(QD)^2(qD)^2$ term which we neglect in this approximation with respect to the $(QD)^2$ term of Eq. (F19), and a $(qD)^2$ term. Thus, using Eqs. (F12), (F21), (F20), and (F19) in Eq. (F3) we obtain

$$\begin{aligned}\widetilde{G}(q,Q)=&\frac{\mu^2}{D^2}[B_0(\phi)(QD)^2+K_0(\phi)(qD)^4+O(\epsilon)]\\&-\frac{4\mu^2}{D^2}\left[\sum_{k=1}^{\infty}\frac{\sin^2(\pi k\phi)}{k}e^{-\epsilon 2\pi k}-\frac{1}{2}\frac{\gamma}{\mu^2}\right](qD)^2.\end{aligned} \tag{F22}$$

As shown in Appendix G the coefficient of $(qD)^2$ (i.e., the effective line tension) is zero to $O(\epsilon)$ due to the equilibrium condition. Thus, using Eq. (G7) in Eq. (F22), we obtain

$$\widetilde{G}(q,Q)=\frac{\mu^2}{D^2}[B_0(\phi)(QD)^2+K_0(\phi)(qD)^4]+\text{higher order terms in }\epsilon,qD,\text{ and }QD. \tag{F23}$$

APPENDIX G: THE EQUILIBRIUM CONDITION FOR THE STRIPE-PHASE

In this Appendix we derive the equilibrium condition for the stripe phase in an alternative form to that derived in Sec. II. This form is compatible with the calculations in Appendix F and we use it to prove the vanishing of effective line tension for the symmetric modes [see Eq. (F22)].

We rewrite the free energy density of the stripe phase, Eq. (2.4), using the Poisson summation formula and a Gaussian representation for P. The multipole correction [already mentioned after Eq. (A14)] will be introduced at a later stage.

$$P(R)=\tfrac{1}{2}\rho^{-1}=\tfrac{1}{2}(R^2+\Delta^2)^{-1/2}=\frac{1}{\sqrt{\pi}}\int_0^{\infty}dt e^{-(R^2+\Delta^2)t^2}. \tag{G1}$$

The boundary energy per cell [last term of Eq. (A13)] is

$$\begin{aligned}\Delta E_{cell}&=\mu^2\sum_{m=-\infty}^{\infty}\int_{-L/2}^{L/2}\int_{-L/2}^{L/2}dx_1dx_2\\&\quad\times\{P(\sqrt{(m+\phi)^2D^2+(x_1-x_2)^2})+P(\sqrt{(m-\phi)^2D^2+(x_1-x_2)^2})-2P(\sqrt{(mD)^2+(x_1-x_2)^2})\}\\&=\tfrac{1}{2}\mu^2\sum_{m=-\infty}^{\infty}\int_{-L}^{L}d\xi\int_{-\infty}^{\infty}d\eta\{P(\sqrt{(m+\phi)^2D^2+\eta^2})+P(\sqrt{(m-\phi)^2D^2+\eta^2})-2P(\sqrt{(mD)^2+\eta^2})\}\\&=\mu^2L\sum_{m=-\infty}^{\infty}\int_{-\infty}^{\infty}d\eta\{P(\sqrt{(m+\phi)^2D^2+\eta^2})+P(\sqrt{(m-\phi)^2D^2+\eta^2})-2P(\sqrt{(mD)^2+\eta^2})\},\end{aligned}\tag{G2}$$

where $\xi=x_1+x_2$, $\eta=x_1-x_2$, and the limits of the integration over η were taken to $\pm\infty$ due to the convergence of the integral. Using Eq. (G1) and the Poisson summation formula Eq. (E5) in Eq. (G2), we obtain [in the same manner that Eq. (D15) was obtained] the energy per unit length

$$\begin{aligned}\Delta E&=\frac{1}{L}\Delta E_{cell}=\mu^2\int_{-\infty}^{\infty}d\eta\frac{1}{\sqrt{\pi}}\int_0^{\infty}dt\sum_{m=-\infty}^{\infty}e^{-[(2\pi m+2\pi\phi)(D/2\pi)^2+\eta^2+\Delta^2]t^2}+e^{-[(2\pi m-2\pi\phi)(D/2\pi)^2+\eta^2+\Delta^2]t^2}\\&\quad-2e^{-[(2\pi m)^2(D/2\pi)^2+\eta^2+\Delta^2]t^2}\\&=-\frac{4\mu^2}{D}\sum_{k=-\infty}^{\infty}\sin^2(\pi k\phi)\int_0^{\infty}dt\,t^{-1}e^{-\Delta^2t^2-(\pi k/D)^2t^{-2}}\int_{-\infty}^{\infty}d\eta\ \mathrm{e}^{-t^2\eta^2}\\&=-\frac{4\sqrt{\pi}\mu^2}{D}\sum_{k=-\infty}^{\infty}\sin^2(\pi k\phi)\int_0^{\infty}dt\,t^{-2}e^{-\Delta^2t^2-(\pi k/D)^2t^{-2}}\\&=-4\mu^2\sum_{k=1}^{\infty}\frac{\sin^2(\pi k\phi)}{k}\,e^{-\epsilon 2\pi k}.\end{aligned}\tag{G3}$$

The multipole correction [21] is $-\mu^2$ per unit length per boundary to order $O(\epsilon^0)$. Having two boundaries per cell and introducing the microscopic line tension γ the free energy density is written

$$\begin{aligned}\Delta f&=\frac{1}{D}(\Delta E-2\mu^2+\gamma)\\&=-\frac{4\mu^2}{D}\left[\sum_{k=1}^{\infty}\frac{\sin^2(\pi k\phi)}{k}e^{-\epsilon 2\pi k}+\frac{1}{2}\right]+\frac{2\gamma}{D}.\end{aligned}\tag{G4}$$

In order to obtain the equilibrium condition we minimize Δf with respect to D and find

$$0=\frac{\partial(\Delta f)}{\partial D}=-\frac{\Delta f}{D}+\frac{\partial(\Delta f)}{\partial\epsilon}\frac{\partial\epsilon}{\partial D}=-\frac{\Delta f}{D}-\frac{4\mu}{D^2}S,\tag{G5}$$

where

$$\begin{aligned}S&=2\pi\epsilon\sum_{k=1}^{\infty}\sin^2(\pi k\phi)e^{-\epsilon 2\pi k}\\&=\pi\epsilon\left[\frac{1}{e^{2\pi\epsilon}-1}-\frac{1}{2}\frac{\cos(2\pi\phi)-e^{-2\pi\epsilon}}{\cosh(2\pi\epsilon)-\cos(2\pi\phi)}\right]\\&=\tfrac{1}{2}+O(\epsilon^2).\end{aligned}\tag{G6}$$

The sum was calculated by representing the sine in terms of exponents, thus obtaining a geometric series which can be summed exactly. Using Eqs. (G4) and (G6), the equilibrium condition, Eq. (G5), is rewritten to order $O(\epsilon^0)$

$$\frac{4\mu^2}{D^2}\left[\sum_{k=1}^{\infty}\frac{\sin^2(\pi k\phi)}{k}e^{-\epsilon 2\pi k}-\frac{1}{2}\frac{\gamma}{\mu^2}\right]=0.\tag{G7}$$

Note that ϵ in the argument of the exponent plays a role of a natural cutoff. The sum in Eq. (G7) diverges in the limit $\epsilon\to 0$ and it is therefore necessary to keep a finite value of ϵ to maintain convergence. This has the result that the equilibrium quantities depend on the cutoff, as indeed was found in Eqs. (2.5).

APPENDIX H: THE KERNEL FOR THE ANTISYMMETRIC MODES

In this Appendix we calculate the kernel $G_a(q)$ for the fluctuation Hamiltonian of the antisymmetric modes of one stripe in the supercrystal (see Fig. 4). The rest of the stripes are assumed to be at their equilibrium position (i.e., a mean field approximation). Without affecting the generality, we choose the stripe labeled 1 in the zeroth cell. Using the no-

tation of Eq. (D1) we have

$$Y(q,i\neq 0)=(0,0); \quad Y(q,0)=y_0(q)(-1,1), \tag{H1}$$

where $Y(q,i)$ is a row vector, whose two components are the ith cell boundary displacements in Fourier space. Thus, $2y_0(q)$ is the Fourier transform of the local change in the width of the stripe. Equation (D1) is rewritten

$$\Delta E_{dip}=\frac{1}{2}\sum_q |y_0(q)|^2 G_d(q), \tag{H2a}$$

where

$$G_d=\mathscr{C}_{1,1}(q,0)+\mathscr{C}_{2,2}(q,0)-\mathscr{C}_{1,2}(q,0)-\mathscr{C}_{2,1}(q,0). \tag{H2b}$$

An explicit calculation of $\tilde{V}(q,w)\equiv\int_{-\infty}^{\infty} du(u^2+w^2+\Delta^2)^{-(3/2)}e^{iqu}$ gives

$$\tilde{V}(q,w)+\tilde{V}(-q,w)=\frac{4q}{w'}K_1(qw');$$

$$\tilde{V}(0,w)=\frac{2}{w'^2}, \tag{H3}$$

where $K_1(x)$ is the modified Bessel function of order 1. To $O((\Delta/D)^0)$ we have $w'=w$ for $w\gg\Delta$ and $w'=\Delta$ for $w=0$ [35]. Using Eq. (H3) in the definition of $\mathscr{C}_{m,n}$ in Eq. (D2), Eq. (H2b) is rewritten

$$G_d=\mu^2\left\{\frac{1}{D^2}\sum_{p=1}^{\infty}\left[\frac{1}{(p-\phi)^2}+\frac{1}{(p+\phi)^2}-\frac{2}{p^2}\right]+\frac{1}{D_1^2}-\frac{1}{\Delta^2}+q\left[\frac{K_1(q\Delta)}{\Delta}+\frac{K_1(qD_1)}{D_1}\right]\right\}. \tag{H4}$$

The first two sums are rewritten

$$\sum_{p=1}^{\infty}\left[\frac{1}{(p-\phi)^2}+\frac{1}{(p+\phi)^2}\right]=-\frac{d^2}{d\phi^2}\sum_{p=1}^{\infty}\ln\left(1-\frac{\phi^2}{p^2}\right)=-\frac{d^2}{d\phi^2}\ln[\mathrm{sinc}(\pi\phi)]=\phi^{-2}[\mathrm{sinc}^{-2}(\pi\phi)-1]. \tag{H5}$$

Substituting $\Sigma_{p=1}^{\infty}p^{-2}=\pi^2/6$ and Eq. (H5) for the sums in Eq. (H4) we find

$$G_d(q)=4\mu^2\left\{D_0^{-2}[1-\tfrac{1}{3}\sin^2(\pi\phi)]+q^2\left[\frac{K_1(q\Delta)}{q\Delta}-\frac{1}{(q\Delta)^2}+\frac{K_1(qD_1)}{qD_1}\right]\right\}, \tag{H6}$$

where D_0 is the equilibrium stripe width for surface fraction $\phi\to 0$. Using Eq. (2.5b), D_0 is defined

$$D_0=\lim_{\phi\to 0}D_1=\Delta e^{\gamma/\mu^2}. \tag{H7}$$

Adding to the boundary energy the microscopic (short-ranged) attractions through the line tension γ, we find the fluctuation Hamiltonian for the antisymmetric modes for one stripe,

$$\Delta H_a=\frac{1}{2}\sum_q |y_0(q)|^2 G_a(q), \tag{H8}$$

where

$$G_a(q)=G_d(q)+2\gamma q^2=4\mu^2\left\{D_0^{-2}[1-\tfrac{1}{3}\sin^2(\pi\phi)]+q^2\left[\frac{K_1(q\Delta)}{q\Delta}-\frac{1}{(q\Delta)^2}+\frac{K_1(qD_1)}{qD_1}+\frac{1}{2}\frac{\gamma}{\mu^2}\right]\right\}. \tag{H9}$$

[1] C. M. Knobler, J. Phys. Condens. Matter **3**, S17 (1991).
[2] H. Möhwald, R. M. Kenn, D. Degenhardt, K. Kjaer, and J. Als-Nielsen, Physica A **168**, 127 (1990).
[3] M. Seul and M. J. Sammon, Phys. Rev. Lett. **64**, 1903 (1990).
[4] T. Garel and S. Doniach, Phys. Rev. B **26**, 325 (1982).
[5] D. Andelman, F. Broçhard, and J-F Joanny, J. Chem. Phys. **86**, 3673 (1987).
[6] H. M. McConnell and V. T. Moy, J. Phys. Chem. **92**, 4520 (1988).
[7] M. Seul and D. Andelman, Science **267**, 476 (1995).
[8] For analysis of effects of in-plane dipolar moments see, for example, P. Muller and F. Gallet, J. Phys. Chem. **95**, 3257 (1991).
[9] T. M. Fischer, R. F. Bruinsma, and C. M. Knobler, Phys. Rev. E **50**, 413 (1994).
[10] K-O Ng and D. Vanderbilt (private communication).
[11] D. Andelman, F. Broçhard, C. Knobler, and F. Rondelez, in *Micelles, Membranes, Microemulsions, and Monolayers*, edited by W. Gelbart *et al.* (Springer-Berlag, New York, 1994), Chap. 12, p. 586.
[12] D. J. Keller, H. M. McConnell, and V. T. Moy, J. Phys. Chem. **90**, 2311 (1986).
[13] D. Sornette, J. Phys. (Paris) **48**, 151 (1987).
[14] D. Sornette, J. Phys. (Paris) **48**, 1413 (1987).
[15] J. Toner and D. R. Nelson, Phys. Rev. B **23**, 316 (1981).
[16] H. M. McConnell, J. Phys. Chem. **96**, 3167 (1992).
[17] A. Cebers (private communication).
[18] R. de Koker, W. Jiang, and H. M. McConnell, J. Phys. Chem. **99**, 6251 (1995).
[19] Ar. Abanov, V. Kalatsky, V. L. Pokrovsky, and W.M. Saslow, Phys. Rev. B **51**, 1023 (1995).
[20] L. Golubović and Z-G Wang, Phys. Rev. E **49**, 2567 (1994).
[21] H. M. McConnell and R. de Koker, J. Phys. Chem. **96**, 7101 (1992).
[22] An exact calculation shows that the correspondence between the two approaches is $a\leftrightarrow(e/2)\Delta$ for the evaluation of the

line integrals, and $a \leftrightarrow \Delta$ for the evaluation of the energy densities ϵ_i. However, this difference is irrelevant for our calculations since the ϵ_i terms are taken as the zero of energy and will be discarded in the analysis of both equilibrium and fluctuations of the stripe phase.

[23] C. Flament and F. Gallet, Europhys. Lett. **20**, 331 (1992).

[24] M. Seul and V. S. Chen, Phys. Rev. Lett. **70**, 1658 (1993).

[25] W. Helfrich, Z. Naturforsch. Teil A **33**, 305 (1978).

[26] P. M. Chaikin and T. C. Lubensky, *Principles of Condensed Matter Physics* (Cambridge University Press, New York, 1995), Chap. 6, p. 298.

[27] P.G. de Gennes and J. Prost, *The Physics of Liquid Crystals*, 2nd ed. (Clarendon, Oxford, 1993), Chap. 9, p. 490.

[28] S. T. Chui and J. D. Weeks, Phys. Rev. Lett. **40**, 733 (1978).

[29] S. A. Safran, *Statistical Thermodynamics of Surfaces, Interfaces, and Membranes* (Addison-Wesley, 1994), Chap. 3, p. 92.

[30] See, for example, S. A. Safran, *Statistical Thermodynamics of Surfaces, Interfaces, and Membranes* (Ref. [29]), Chap. 2, p. 61.

[31] Y. Saito, Z. Phys. B **32**, 75 (1978).

[32] The self-consistent calculation suggests a possible first-order roughening transition in systems with only short-range interactions. See A. Deutsch and S. A. Safran (unpublished).

[33] See, for example, G. Arfken, *Mathematical Methods for Physicists* (Academic Press, Orlando, FL, 1985), Chap. 1, pp. 58, 59.

[34] A more rigorous analysis of the microscopic cutoff (but with similar results) is done by S. A. Langer, R. E. Goldstein, and D. P. Jackson, Phys. Rev. A **46**, 4894 (1992).

[35] Note that there is no intermediate case, since the stripes are assumed to be much thicker than the microscopic size Δ for our model to be self-consistent.

[36] M. J. Lighthill, *Introduction to Fourier Analysis and Generalized Functions* (Cambridge University Press, New York, 1958), Chap. 5, p. 67.